UNIVERSITY OF OKLAHOMA

GRADUATE COLLEGE

Analysis and Application of Virtual-Flow Meter Technology for Chiller-Water Valve and Outside-Air Controls

A THESIS

SUBMITTED TO THE GRADUATE FACULTY

In partial fulfillment of the requirement for the

Degree of

MASTER OF SCIENCE

By

Marwan Hashem

Norman, Oklahoma

2022

Downloaded from SHAREOK. Persistent Handle URL: https://hdl.handle.net/11244/335537

Analysis and Application of Virtual-Flow Meter Technology for Chiller-Water Valve and Outside-Air Controls

A THESIS APPROVED FOR THE

SCHOOL OF AEROSPACE AND MECHANICAL ENGINEERING

BY THE COMMITTEE CONSISTING OF

Dr. Li Song, Chair

Dr. Wilson Merchan-Merchan

Dr. Jie Cai

© Copyright by Marwan Hashem 2022

All Rights Reserved.

Acknowledgment

In the name of Allah, the entirely merciful, the especially merciful, I want to acknowledge the many people that helped me throughout my master's journey. Firstly, I would like to express my sincere gratitude to my faculty advisor, Dr. Li Song, who provided endless support throughout this project. Since joining her HVAC class and approaching her regarding her research, she has seen my potential to develop in her research and specifically this field. Despite her faculty researcher status, she is, more importantly, an educator to me and others. Her guidance and mentoring pushed me to grow academically, professionally, and personally. I have had the opportunity to engage in projects other than my own, where she always ensured a fruitful experience. She will always remain the spark to my master's completion and the start of my professional journey.

Secondly, I would like to thank Dr. Gang Wang, a faculty researcher at the University of Miami. As part of a joint research project, he always showed a willingness to provide informational support regarding my work. Also, thanks to my committee members: Dr. Wilson Merchan-Merchan and Dr. Jie Cai, for providing encouragement and constructive feedback during my defense.

Last but not least, I would like to attribute this success to my parents and brother, that have given me endless support and resources to make this journey possible, especially under the hardship of being an international student. These thanks also extend to my dear friends for providing the secondary support after my family.

Table of Contents

Acknowledgment iv

List of Figures vii

List of Tables x

Nomenclature xi

Abstract xii

Chapter 1 : Introduction 1

1.1 Background 2

1.2 Problem Statement and Proposed Solution 4

1.2.1 Outdoor Air VFM 5

1.2.2 Chiller Water Valve VFM and Cascade Control 5

1.3 Thesis Breakdown 6

Chapter 2 : Review of State of Art 8

2.1 Virtual Flow Meter 9

2.2 Chiller Water Virtual Flow Meter 10

2.2.1 Review of Cascade Control 11

2.3 Outdoor Air Virtual Flow Meter 14

2.4 Limitations and Research Questions 17

Chapter 3 : Methodology 21

3.1 Experimental and Mathematical Models 21

3.1.1 CHW-VFM 21

3.1.2 Cascade Control 24

3.1.3 OA-VFM 26

3.2 Test Design 27

3.4 Testing Layout 32

3.4.1 Operational Background 32

3.4.2 Test Bed 35

Chapter 4 : Results and discussion 43

4.1 CHW-VFM Performance Analysis 43

4.2 Cascade Control Performance Analysis 50

4.2.1 Operation under Low Load Condition 50

4.2.2 Operation under High Load Condition 52

4.3 Outdoor Air VFM 55

Chapter 5 : Conclusion and Future Work 66

References 68

List of Figures

Figure 1-1 Air conditioning breakdown based on electricity demand [2] 1

Figure 1-2 Layout of the Cascade controller used for chiller water loop operation 4

Figure 2-1 Traditional layout of sensors used in HVAC control operations [16] 8

Figure 2-2 Types of virtual sensors [10] 10

Figure 2-3 Development of VFM for refrigerants in HVAC by Li et al. [10] 10

Figure 2-4 Operation principle of PID controller [22] 12

Figure 2-5 Supply air and room air temperature performance 1) Single control 2) Cascade control [12] 12

Figure 2-6 Supply air VFM developed by Wang et al. [31] 15

Figure 2-7 Inputs of mixing chamber model developed by Tan et al. [30] 16

Figure 3-1 Layout of CHW valve and cooling coil and their corresponding DP [19] 22

Figure 3-2 The layout of the proposed cascade control 25

Figure 3-3 Layout of single control model used for cascade comparison study 25

Figure 3-4 Operation template of the CHW-VFM "B" integrated into the cascade control "A" . 29

Figure 3-5 Basic layout of traditional AHU 33

Figure 3-6 The AHU used for the experimental study. 36

Figure 3-7 The Ultrasonic meter used for CHW flow a) Module b) Transducers mounted on the CHW intake pipe 37

Figure 3-8 Duct Traverse performed for outdoor airflow measurements 39

Figure 3-9 The chilled water valve used in the experiment 40

Figure 3-10 Differential pressure sensors installed to measure ΔP_L 40

Figure 3-11 An overview of the VYKON N4 readings recorded by the system's controller. 41

Figure 3-12 HOBO data logger installed to measure T_{MA}, CHW-valve command, CHW-valve feedback, and T_{SA} 42
Figure 4-1 Valve command and feedback signal of valve position step changes performed..... 43
Figure 4-2 Chilled water flow rate vs. valve opening % measured using the ultrasonic meter.... 44
Figure 4-3 Valve dead-band experience at command signals larger than 95%..... 44
Figure 4-4 Valve gain (K_v) associated with each valve position..... 45
Figure 4-5 Valve flow coefficient (C_v) vs. the valve command signal..... 46
Figure 4-6 Valve characteristics curve divided into four linear segments..... 47
Figure 4-7 Chilled water flowrate measured by the ultrasonic meter and the built VFM with STD values 49
Figure 4-8 Chilled water flow measurement using VFM and ultrasonic meter nearing its maintenance due time. 49
Figure 4-9 Cascade and single controller performance for T_{SA} set point step change under low load conditions..... 51
Figure 4-10 Cascade and single controller performance for DP step change under low load conditions..... 52
Figure 4-11 Cascade and single controller performance for T_{SA} step change under high load conditions..... 53
Figure 4-12 Cascade and single controller performance for DP step change under high load conditions..... 53
Figure 4-13 Estimation and measurement of outdoor air vs. ΔT for one-week sample size..... 56
Figure 4-14 OA ratio measurement vs. estimation for ΔT = 20F° – 30F° 57
Figure 4-15 Estimation and measurement of outdoor air vs. ΔT for one-week sample size..... 58

Figure 4-16 Estimation and measurement of outdoor air ratio for ΔT (F°) = 40 - 50 60

Figure 4-17 OA damper position and OA ratio values 61

Figure 4-18 OA damper position and OA ratio values under constant systems airflow rate 62

Figure 4-19 OA ratio vs. damper position 62

Figure 4-20 OA ratio and supply fan head at different supply airflow rates 64

Figure 4-21 Trendlines of OA ratio correlations with damper position at different supply airflow rates 64

List of Tables

Table 3-1 Details of the test cases performed for the cascade control study 30

Table 4-1 Equations of characteristics curve linear segments and their operating range 48

Table 4-2 Mean values and uncertainty analysis for each test 2 study cases 54

Table 4-3 Mean relative error values of the different ΔT ranges for the one-month sample size 57

Table 4-4 Mean relative error values of the different ΔT ranges for the one-week sample size .. 59

Nomenclature

VFM	Virtual flow meter
AHU	Air handling unit
BAS	Building automation system
CAV	Constant air volume
CFM	Cubic feet per minute
CHW	Chilled water
Cmd	Command
DCV	Demand control ventilation
Dmp	Damper
DP	Differential pressure
FDD	Fault detection and diagnosis
OA	Outdoor air
PID	proportional integral derivative
TMA	Mix air temperature
TOA	Outdoor air temperature
TR	Terminal box
TRA	Return air temperature
TSA	Supply air temperature
VAV	Variable air volume
VFD	Variable frequency drive
STD	Standard deviation

Abstract

The following work focuses on using virtual flow meters (VFM) for HVAC controls and how they can replace physical sensors to reduce cost and increase efficiency. The study focuses on implementing VFM to measure outdoor air (OA) intake and the cooling coil chiller water flow rate. As HVAC controls advance with time, OA flow measurements became crucial to precisely maintain building pressurization, building codes, and healthy air quality for occupants. Moreover, Chiller water (CHW) flowrate measurement is essential for detecting inefficiencies in the cooling system and maintaining a stable supply air temperature. Consequently, newer systems utilize physical flow meters despite their high initial cost, whereas older systems do not. Outdoor air and chilled water VFM will help lower initial cost and improve HVAC controls which can increase efficiency and lower operation cost overall. Cascade control was also investigated to improve HVAC controls by integrating it with CHW-VFM. Thus, VFM will also eliminate the systematic error associated with hardware maintenance. Using an experimental air handling unit (AHU), both VFM were implemented and tested for their performance. The CHW-VFM had a percentage error of less than 5% compared to a physical ultrasonic meter. Also, cascade control operation has increased performance compared to a single control operation in maintaining supply air temperature under various disturbances. Also, the suggested cascade control VFM covers a larger range of operating conditions, eliminating the need for seasonal resets. In addition, It was found that the OA ratio can be estimated when (T_{RA} - T_{OA}) > 6 °F with a relative error of less than 8%. Also, a correlation between the outdoor air damper position and OA ratio can be established if mixing chamber pressure is maintained steadily.

Chapter 1 : Introduction

The past two decades have faced an increase in HVAC units' installations due to rising temperatures resulting from climate change. According to Todd Bluedorn, Lennox International's CEO, air conditioning operated 30% higher in 2021 compared to 2020. He also added that the weather had been 5 percent hotter from 2016 to 2020, which not only did it increase the demand for new installations but to replacement units [1]. Consequently, HVAC owners are prone to higher electricity costs which have sparked the need for newer HVAC controls and technologies.

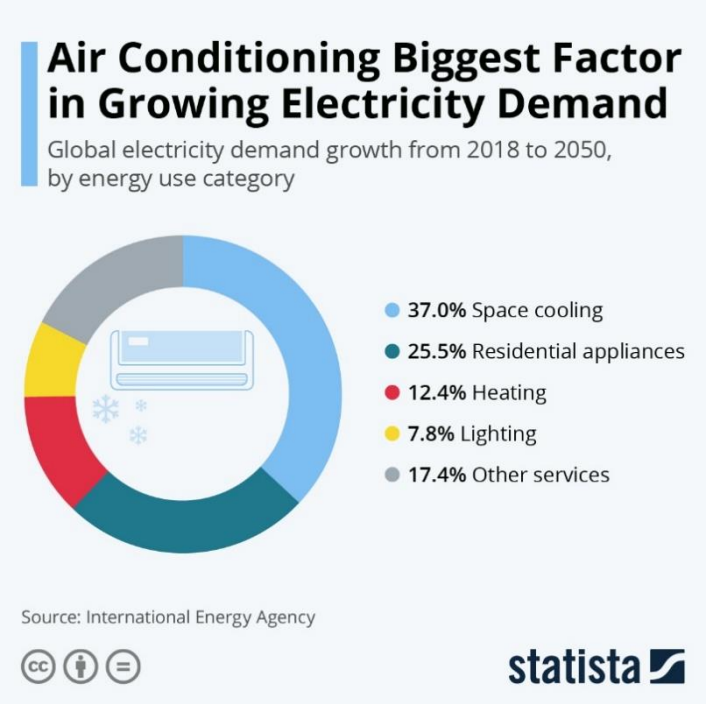


Figure 1-1 Air conditioning breakdown based on electricity demand [2]

1.1 Background

Using newer controls, HVAC units became more efficient and optimized to lower operating times and associated costs [3]. As HVAC design needs to satisfy building codes and air quality standards, the need for new systems is required. For example, a typical HVAC residential unit does not include an outdoor air intake mechanism like larger commercial and office-sized air handling units [4]. However, higher outdoor air intake is required due to the increased demand for higher air quality in buildings and especially with the global spread of SARS-CoV-2 [4]. As a result, advanced residential units started featuring conditioned outdoor air. In addition, the department of homeland security has called for additional outdoor air dilution to fight the spread of SARS-CoV-2.

Traditionally, outdoor airflow can be measured using a physical flow sensor mounted in the outdoor air intake, or it can be calculated using other measured temperature readings from the systems' temperature sensors (i.e., outside, return and mix temperatures) [5]. In addition, physical flow measurements can consist of velocity and pressure sensors to calculate the flow rate in a commonly used method called Duct Traverse. This method requires using multiple sensors laid out evenly over a cross-sectional area of a straight duct. However, sensors do not only increase the initial cost of the systems, but they are not always feasible to implement where not enough straight ducting is found [6].

Moreover, the physical sensor's reading becomes inaccurate over time due to deterioration caused by external weather factors such as extreme cold and heat. This deterioration can increase the sensor's error, reducing the system's potential savings or compromising the thermal comfort spaces. Unlike other airflow sensors, outdoor airflow sensors have been linked to providing the highest operational cost savings due to their accuracy in measuring minimum outdoor air intake

during hot seasons, leading to lower cooling loads [7]. Thus, the benefits of using a physical flow meter are connected to its reading accuracy.

Research has not only focused on decreasing the overall costs of the HVAC systems, but it also focused on optimizing its performance for a faster operation time. Traditionally, HVAC research focuses on building dynamics and their effect on HVAC operations. These dynamics include the cooling and heating equipment [8]. Chiller water dynamics constitute an essential factor in the cooling operations where most commercial buildings utilize chilled water loops to provide cooling in a traditional AHU. As supply temperature relies on the supply chilled water temperature, optimizing the chilled water loop and its associated variables will result in a stable supply temperature. A supply air temperature of 55 F° is currently considered the standard discharge temperature in HVAC units to maintain thermal comfort and operation efficiencies [9]. As a result, the dynamic changes in the chiller water loop will result in changes to the supply air temperature, which is not desired to maintain thermal comfort. Studies were made to understand the dynamic changes of cooling loops and chilled water plants and how to improve their efficiency.

Despite the importance of cooling loops in HVAC operations, air handling units do not rely on the chiller water loop to maintain a set supply temperature. Instead, they utilize a variable flow operation controlled using a flow actuator known as chiller water valves. This controlled valve will open and close to restrict the flow of chilled water into the cooling coil based on cooling demands. Consequently, optimization of the valve controls will enhance the system's performance by maintaining a stable 55 F° supply temperature. However, such control requires using a flow meter to measure the chilled water flow rate of the cooling coil, which will increase the initial installation cost like the OA flow sensor. In addition, some physical flow meters

require an invasive installation that might not be feasible in smaller systems where not enough space is found. Therefore, a VFM is also being developed to measure water flow rate using other measuring system variables without a physical sensor [10].

Cascade control has been suggested to improve control performance by eliminating the influences of external factors during regular operations. The cascade control relies on using two controllers. The first controller is a primary outer control loop that maintains the output of supply air temperature to its specified setpoint as a function of the chilled water rate setpoint. This controller considers the error produced by the supply air output based on the chilled-water flow gains at different operating conditions -low and high (design) loads. The second controller operates as an inner loop to control the output of chilled water flow rate as a function of the chiller water valve command with reference to the chilled water flow setpoint outputted by the primary controller.

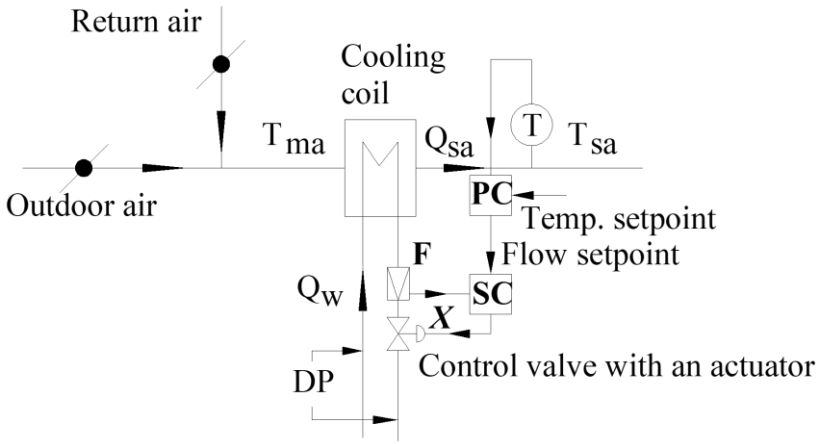


Figure 1-2 Layout of the Cascade controller used for chiller water loop operation

1.2 Problem Statement and Proposed Solution

Despite the advancement in HVAC controls and the direct impact on increased performance and lower operation costs, this has consequently raised the initial installation cost associated with the

need for high-quality sensors. Without these physical sensors, these controls cannot be implemented.

1.2.1 Outdoor Air VFM

Outdoor air operations generally require a flow sensor to be in place to compute the outdoor air ratio of the system's supply air to meet thermal comfort and health standards. This flow measurement is also necessary for OA damper controls to ensure that the required ratio is supplied from the outside. As damper operations use an actuator operating from 0% to 100% position, this position dynamically changes to meet the required OA flow rate setpoint and does not usually correspond to a fixed OA ratio [5]. By modeling the operation of the OA damper and the OA flow rate, we can construct a virtual flow meter using a regressed correlation between damper position and OA ratio. The correlation is obtained by outdoor air, mixed air, and return air temperatures when the temperature difference between the return air and outdoor air is large enough to eliminate the impacts of the measurement errors. This VFM can replace the need for a physical flow meter in HVAC operation. Ultimately, it will reduce the initial installation cost of a physical sensor and enhance demand control ventilation (DCV).

1.2.2 Chiller Water Valve VFM and Cascade Control

Similarly, a virtual flow meter will also be tested to measure the chilled water flow rate as a function of valve position and differential pressure across the cooling coil [11]. This VFM will eliminate the need to use a physical sensor, reducing the initial installing cost and maintenance cost associated with periodic calibration. As the current state of the art VFM has demonstrated a low level of uncertainty that can replace a physical flow meter, this research also tests the ability to improve the VFM performance using cascade control. Under regular operation, valve control utilizes a single loop controller consisting of a traditional proportional-integral (PI) controller,

which will use the supply air temperature and setpoint as its input and reference point. However, as single controllers come with tuned parameters based on design conditions, they cannot account for the system's gain changes because of disturbances, making them more sensitive under abnormal conditions [12]. It is proposed that using a cascade control for the valve operation will result in faster system performance and more stable supply air temperature under system disturbances such as the chiller loop varying pressures. Cascade control has shown to be stable with varying system gains, as is the case for cooling coil operations.

1.3 Thesis Breakdown

This research aims to model, design, and test a virtual flow meter for outdoor air and chiller water valve intake using existing measured variables in the building automation system (BAS). The research scope will include the VFM modeling procedure using empirical values obtained during regular operation. Following, the design procedure will be based on the current state-of-the-art research and include control enhancements using cascade control integration. The VFMs will be tested under everyday conditions using an experimental air handling unit used for research purposes, which will then be validated against an existing physical flow meter to ensure accuracy and precision. Consequently, the breakdown of this thesis will be as follows:

Chapter 1: In this chapter, an introduction to the project is given. It demonstrates basic knowledge of HVAC operations and its importance to both the system's performance and its relevance to our everyday lives. It also presents the proposed solution and its relevance finishing with a breakdown of the thesis.

Chapter 2: This chapter discusses the relevance of virtual flow meters to HVAC operations. It demonstrates the financial and performance benefits associated with the use of VFM in HVAC

controls. It also investigates research done in this field and their prospective progress by demonstrating state-of-the-art techniques used to develop VFM.

Chapter 3: This chapter discusses the testing layout used for this experimental study. It includes details about the systems used with a background on its traditional operation. It also includes models used for the experimental study and testing details.

Chapter 4: This chapter presents the results obtained in Chapter 3. Analysis of the results is also discussed and the suggestions made toward the results relevant to the development of chilled water and outdoor air virtual flow meters and their performance in HVAC controls.

Chapter 5: This chapter includes the thesis summary and presents the concluded results and suggestions. It also discusses work limitations and future work needed.

Chapter 2 : Review of State of Art

Due to the complexity of building structures and the need for innovative HVAC designs that operate at a multizone level, control has become a crucial part of guaranteeing an efficient, low-cost operation. A comprehensive, integrated control system is needed, which has shown to provide greater efficiency and lower energy costs [13]. Thus, HVAC controls layered the foundation for efficient building systems.

HVAC systems can come with several control loops. Those loops can be related to a rule-based heuristic control in which standardized protocols and setpoints are performed based on specific input variables. Such controlled operation can be seen in variable air volume systems, where airflow -bounded by the design setpoints- is supplied based on occupancy and temperature inputs [14]. Those inputs are traditionally provided using occupancy and temperature sensors mounted at each zone to provide a dynamic response based on demand. This control has resulted in a significantly lower operating cost than constant air volume (CAV) systems [15].

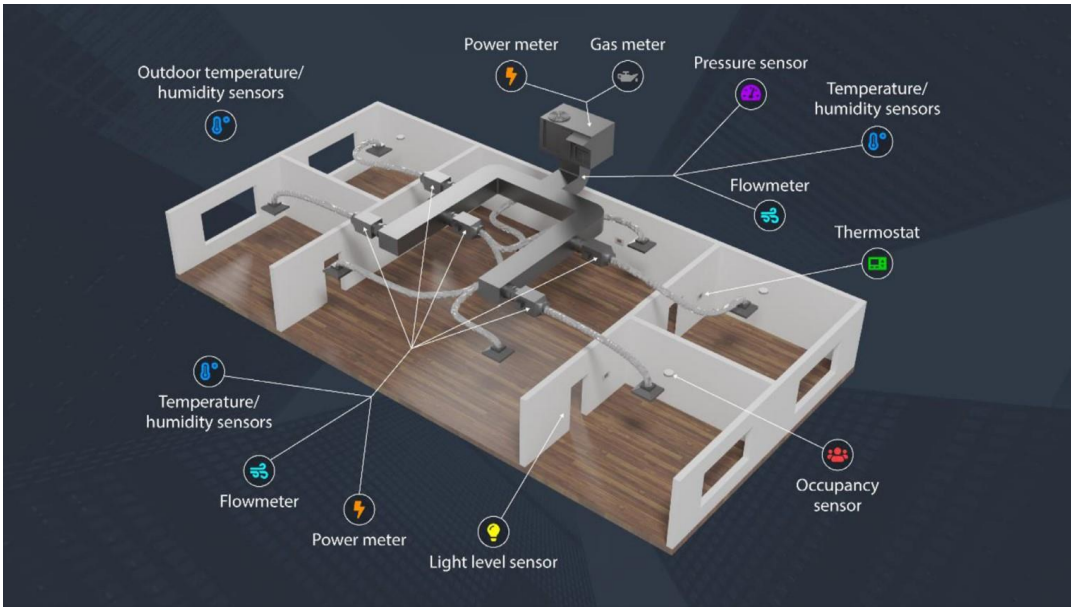


Figure 2-1 Traditional layout of sensors used in HVAC control operations [16]

As such, the HVAC control operation is referred to as a loop. Each control loop consists of one measured variable inputted into a control model that will compute the actions needed to meet the variable set point [16]. As a result, control loops require at least one sensor to measure the targeted value.

Although VAV's present-worth cost is lower than CAV, the initial cost of VAV systems is still higher due to the use of sensors and labor associated with installation [15]. Also, the annual operation cost comes at a higher cost due to the sensor's periodic maintenance that, if not performed, will result in sensors error readings. Lu *et al*. showed in a study that despite the savings associated with using sensors and controls, sensor error could result in up to 16.90% deviation rate for HVAC annual energy consumption and 94.32% deviation rate for outdoor air operation. Thus, they suggested that the outdoor airflow sensor's accuracy primarily impacts potential energy savings compared to other zone-level airflow sensors [7].

2.1 Virtual Flow Meter

Virtual sensors have been modeled and used to reduce the associated hardware and maintenance costs [16]. The use of virtual meters can help reduce operating costs associated with physical sensor reading errors. As a result, much research is focused on developing VFM with a high level of accuracy compared to physical ones.

A Virtual meter is a method used to measure a quantity in a non-invasive manner using a combination of mathematical models that rely on other measured quantities, also known as "Soft Sensors" [10]. Soft sensors have dominated several industries in the past decades, especially the automotive industry, where it has enabled the measurement of complex variables that could not be used with physical sensors [17].

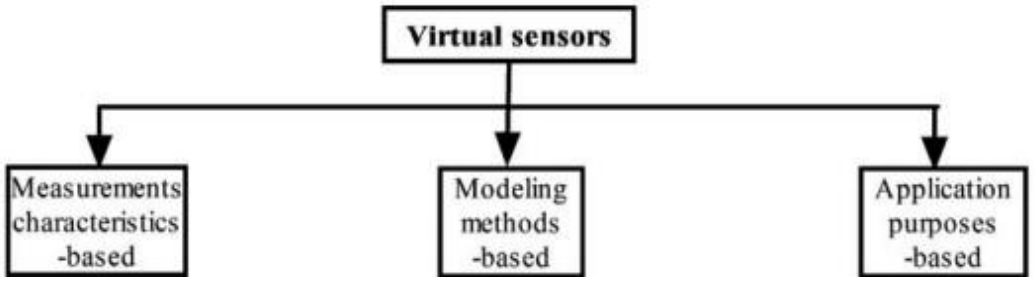


Figure 2-2 Types of virtual sensors [10]

As virtual sensors develop over time, their use in building automation and HVAC-R systems became apparent. For example, Li *et al*. proposed more than five virtual sensors used in fault diagnosis (FDD) of vapor compression air conditioners in their paper. Their sensors were able to measure quantities such as power consumption, refrigerant flow, and evaporation temperatures. In addition, they found that refrigerant flow can be virtually correlated with the compressor's volumetric efficiency with a good level of accuracy using empirical coefficients. Consequently, Li and Braun were able to implement a low-cost multi FDD tool using nine temperature sensors, two pressure sensors, and one humidity sensor [18].

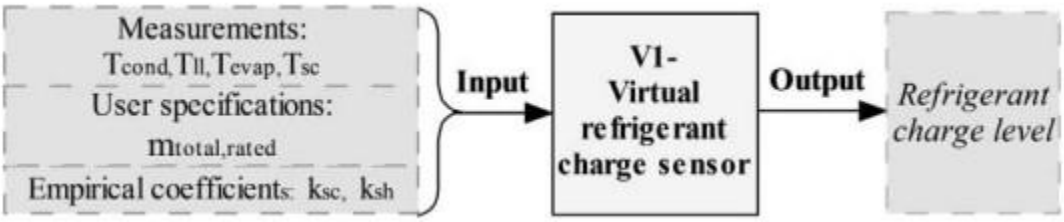


Figure 2-3 Development of VFM for refrigerants in HVAC by Li et al. [10]

2.2 Chiller Water Virtual Flow Meter

In work reported by Song *et al.*, a virtual flow meter for an AHU was introduced using a chiller water control valve. The VFM measured the valve flow as a function of differential pressure and valve command. The work of Song also modeled the loop resistance coefficient curves

associated with the valve position, which provided positive results in determining the valve characteristics [19].

Another study by Song *et al.* investigated the uncertainty associated with the developed VFM by comparing its value to experimental data obtained from an ultrasonic flow meter. The study showed that the VFM had an uncertainty of 1.46% or less with a 95% confidence. Song also suggested that the model of the valve characteristics curve is only accurate when using the empirically determined valve characteristics curves [11].

Modeling of virtual flow meters is not only measured at a pump level but it can also be measured at a chiller level where thermodynamic quantities are used [20]. Zhao *et al*. developed a VFM to measure chiller water in both condenser and evaporator coils. Experimental testing proved to accurately measure flow rate using readily available quantities such as the inlet and outlet temperatures and the refrigerant thermodynamic properties. This model has advanced chiller loop system control by allowing fault detection and diagnosis of chiller loops, thus calculating the chiller's efficiencies and potential energy savings [21].

2.2.1 Review of Cascade Control

Despite the accuracy of developed virtual chiller water flow meters, it is crucial to investigate their performance when operating under traditional control loops. Valve actuation is part of a single control loop that constitutes the chiller water loop. This loop will traditionally utilize a PI or a PID controller under local controlled operations which utilize a supply air temperature sensor as its input variable [12, 16]. However, single controllers are prone to instability due to system changes, making them inadequate in eliminating nonlinearities associated with the coil's and air space thermal capacity [12].

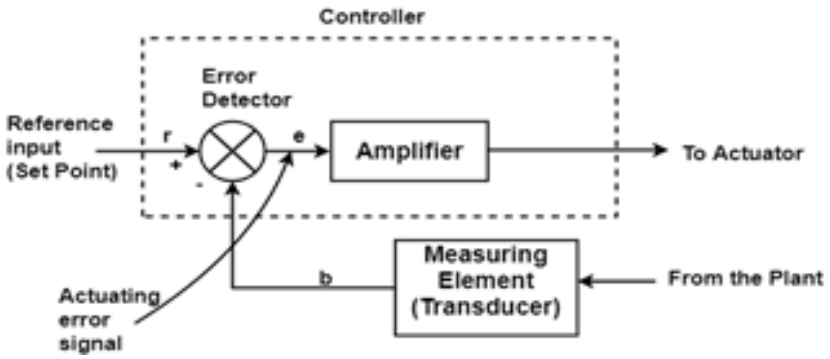


Figure 2-4 Operation principle of PID controller [22]

Cascade control has been introduced to replace single controllers in the HVAC industry due to its higher stability under abnormal system changes. It has improved performance for multiple control loop operations such as chiller water loop and building pressure control [12, 23].

In a study by Phalak *et al*., it was found that the AHU system has nonlinearities associated with the cooling coil performance. He added that single-loop control is only stable at design conditions and is prone to high instability during operating conditions and low chilled flow rate. However, a simulation-based test case showed that cascade control could eliminate a higher instability range than a single controller [12].

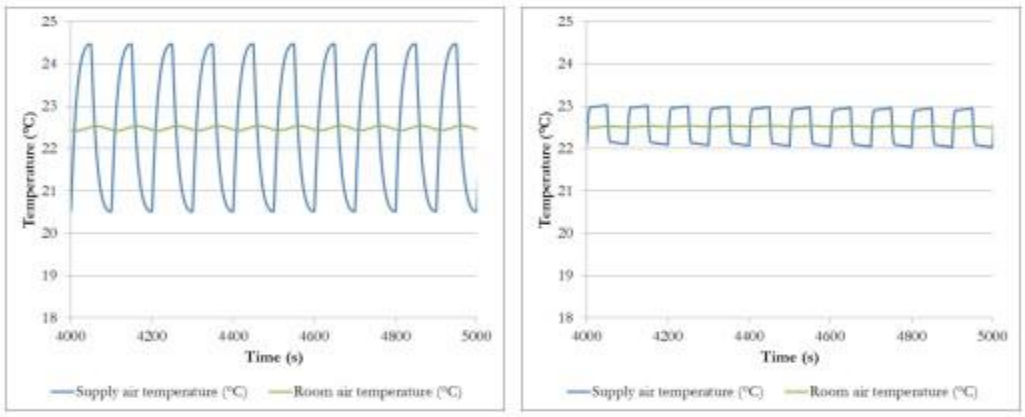


Figure 2-5 Supply air and room air temperature performance 1) Single control 2) Cascade control [12]

Due to the cooling coil's non-linear performance, the AHU can have different gains with varying operating conditions. These changes can call for seasonal controller resets to maintain an efficient performance during a specific range of operating conditions. Thus, cascade control stability can lower seasonal maintenance costs associated with controller gain resets and consumption costs due to extended system operating hours [12].

Due to the nonlinearities associated with HAVC components, such as the cooling coil, PID control with valve actuators have presented large actuator oscillations known as "hunting" [24]. It causes the valve to open and close within a larger range of amplitudes. This phenomenon contributes to reducing the actuator's life span. Also, the regular oscillations cause the system to oscillate downstream and upstream, which will be reflected in the supply air temperature. Consequently, oscillations in the supply air temperature can negatively affect thermal comfort and potential cost savings due to periodic on/off operation.

Price *et al.* showed that the inner loop of the cascade control was able to eliminate actuator hunting by regulating the volume flow rate. He also proposed that cascade control was able to compensate for a large range of HVAC nonlinearities. As a result, cascade control will lower maintenance costs by increasing the actuator's lifespan [24].

Moreover, Hurt *et al.* were able to test cascade control under real operating conditions experimentally. He investigated the controller's stability under supply air temperature, and chiller water loop pressure (DP) changes. He concluded that cascade control had significant performance improvement under DP changes compared to a single loop [25].

In HVAC operation, supply air stability is directly related to DP stability. As multiple AHUs can share a chilled water loop, varying AHU loads can result in DP disturbances due to the variation

of the pump speed. Such disturbances can negatively affect the pump effectiveness and hence reduce potential savings. Thus, the loop needs to deliver the required pressure head to ensure optimum system performance [26].

The cascade control's ability to eliminate the DP effect on supply air will help ensure a stable supply-air temperature under an unstable chiller water loop. Also, it can help reduce DP fluctuations associated with unstable supply air set point temperature as a result of cooling load changes [25].

2.3 Outdoor Air Virtual Flow Meter

Outdoor air operations are essential for ventilation purposes. It is responsible for introducing fresh air to the conditioned space to ensure low levels of carbon monoxide (CO_2). When the economizer is not in operation, the AHU will maintain a minimum outdoor air intake to meet minimum ventilation requirements according to ASHRAE standards [27].

However, the outdoor air intake operation can have significant energy consumption due to higher conditioning loads when the outdoor air temperature exceeds the supply air temperature [28]. Also, the current minimum ventilation rates are usually satisfied using a set outdoor damper position determined upon installation [28]. This practice is due to the lack of a physical outdoor air flow meter because of the high cost, which assumes that the damper position is correlated to the outdoor airflow [5].

A study by Phalak *et al*. has shown that correlating outdoor damper position with flow rate is inaccurate due to pressure and wind speed influences [29]. Thus, without using a static pressure sensor to monitor the mixing air chamber pressure, any variation in pressure will lead to variation in airflow per fixed outdoor position[28]. Therefore, the inaccuracy of using a

minimum damper position can reduce the potential cost savings because it can introduce a higher airflow than required causing a higher conditioning load.

The drawbacks of not using an accurate outdoor airflow meter create limitations for demand control ventilation (DCV). Also, with the increased demand for ventilation rates due to the spread of SARS-Cov-2, the range of damper positions used in outdoor air supply operation is prone to nonlinearities that make it hard to correlate it to the required outdoor air ratio[30].

Efforts to virtually estimate the air flow has been demonstrated to increase potential cost savings for regular operation, decrease initial installation costs due to physical sensors and enhance DCV [29, 30].

In a paper written by Wang *et al.*, his work built a theoretical model to virtually measure the supply air flow rate at an AHU using the fan's head, power, voltage, and frequency as inputs. The model was experimentally tested on an AHU compared to a physical flow meter. It showed a positive match with a standard deviation of 30.1 CFM for a 5-min moving average with a flow range of 950 CFM – 1480 CFM [31].

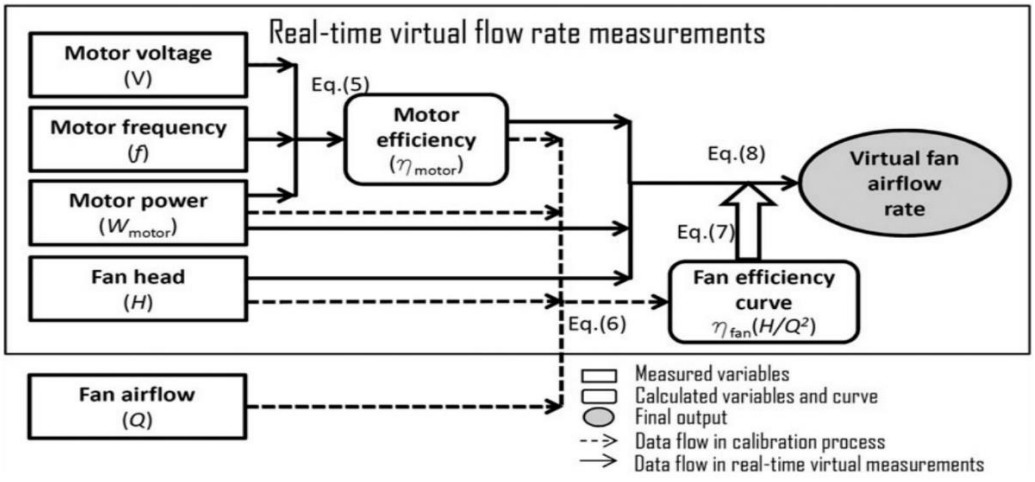


Figure 2-6 Supply air VFM developed by Wang et al. [31]

This virtual supply airflow meter can allow for an inexpensive alternative to using a physical meter with financial and system size constraints. Other papers discussed the ability to virtually measure airflow for return air. For example, Tan *et al*. investigated the relationship between supply, return, and outdoor airflow with respect to control signals from the supply fan and return fan. He found out that supply and return airflow can be linearly estimated using fan signals if the supply fan flow is higher than 40% of its design flow with an error of less than 8%. Moreover, he suggested the ability to estimate outdoor airflow using supply and return airflows and damper position using a mixing chamber model with an accuracy of 3% [30].

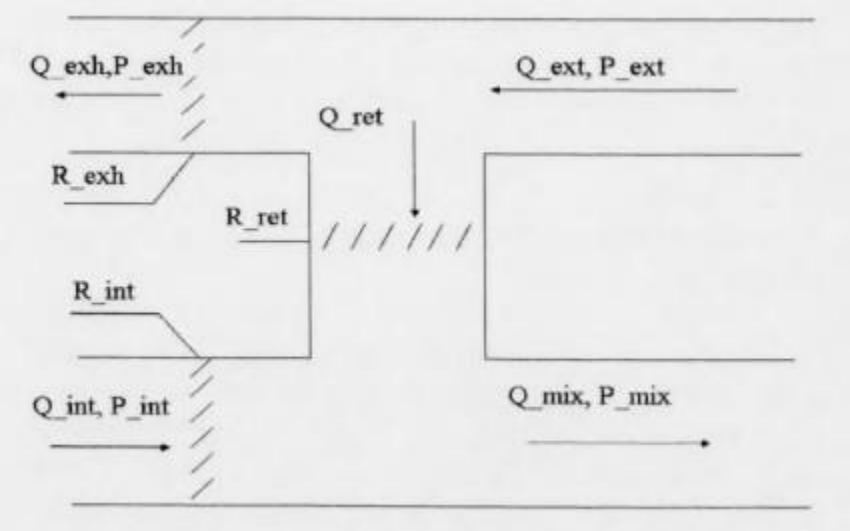


Figure 2-7 Inputs of mixing chamber model developed by Tan et al. [30]

Allowing access to virtual airflow meters for use on AHUs that do not utilize any flow sensors has become easier to implement pressure control inside an AHU, as suggested by Phalak *et al*. Also, the OA-VFM capability of producing outdoor air ratio as a function of temperature variables, using a virtual supply air flow meter can provide an accurate reading of outdoor airflow rate, enhancing demand control ventilation.

Measurements of outdoor airflow can be virtually deduced using the relation between supply airflow rate and outdoor air ratio. The outdoor air ratio can be accurately measured using an energy balance equation that utilizes the mixing chamber temperature measurements [32]. Thus, researchers calculated the outdoor airflow using the outdoor air ratio and readily available readings of the supply flow rate from the building automation system (BAS).

A paper written by Cotrufo *et al.* showed the accuracy of measuring outdoor airflow using a modeled outdoor air ratio meter for AHU in heating mode. He used mixing chamber temperature readings and volumetric airflow rate reading from the BAS to estimate outdoor airflow [32].

However, using the energy balance equation at the mixing box to calculate the outdoor air ratio as proposed by Cotrufo *et al.* can be unreliable under low-temperature differences (T_{RA} -T_{OA}) [28]. As such, significant estimation errors can arise during operations where the temperature difference is not significant, thus causing a decrease in potential cost savings due to inaccurate readings [7].

As positive research was done to develop a robust VFM for supply air, as suggested by Wang *et al.*, the accuracy of developing a virtual outdoor flow meter is still dependent on the accuracy of its input. Therefore, an investigation should be done to study the range at which the outdoor air ratio estimation is accurate and the reliability to correlate it to the damper position.

2.4 Limitations and Research Questions

As demonstrated previously, the use of VFM has proven to provide performance and financial advantages over the use of physical meters. However, despite the efforts to implement estimation methods to develop VFM, there are still research gaps that need to be filled to obtain a greater understanding of virtual sensing.

Despite the research efforts to develop an accurate method of estimating flow in chiller water systems as proposed by Song *et al.*, Zhao *et al.*, and Li *et al.*, the proposed VFM model was tested theoretically in most cases without considering external influences under operating conditions. However, as the chiller water loop has nonlinearities associated with the cooling coil, the VFM might not perform accurately for specific operating ranges[12].

Song *et al*. were able to conduct a performance analysis of the modeled VFM by obtaining experimental results of the valve characteristics. Her model calculated flow rate as a function of DP and valve command. However, the valve command signal might not reflect real-time flow rate due to actuation delays between the valve command and valve feedback and as a result of the valve time constant [33].

The integration of cascade control in the control loop has shown performance advantages by allowing a stable operation under a more extensive range of operating conditions [23]. Also, cascade control eliminated chilled water loop instability due to cooling coil nonlinearities [12]. This was proven experimentally by Hurt *et al.*, where chilled water valve operation became stable under changing DP and supply air temperature setpoints [25].

Therefore, it is proposed that the chilled water virtual meter can be enhanced using cascade control. The cascade control can provide the VFM with a more excellent operating range, eliminating any need for seasonal gain resets, thus reducing maintenance costs for virtual meters. Moreover, the cascade's control ability to maintain a stable supply air temperature in AHU will lead to lower operating costs.

Altogether, the use of chilled water VFM with cascade control will lower installation, operating, and maintenance costs in the long run and provide a faster performance over the use of physical meters and traditional single controllers.

Similarly, the development of a virtual airflow meter has been positive in the last decade to measure supply airflow as presented in Wang *et al.*, and Tan *et al.* Researchers have tried to directly estimate outdoor airflow as a function of OA damper positions. However, the correlation between OA flow and damper position is prone to high error levels due to its high sensitivity to mixing chamber pressure and outdoor wind speed changes.

Tan et al. used a mixing chamber model that considers the mixing chamber to calculate the OA flow rate. However, he was only able to do so under specific operating ranges. His model did require the input of return and supply fan signals and the AHU damper characteristic, which can be hard to obtain if no fan meters are installed. Also, its dependency on fan operation made it only valid under a minimum fan operating condition.

Cotrufo et al. attempted to indirectly measure the OA flow rate by measuring the OA ratio using the energy balance equation and multiplying it by the supply airflow. The study did propose the ability to use supply air VFM but did not use one in their methodology. Their attempt to use the energy balance equation has faced limitations when outdoor air and mixing air temperatures are close in value. The study did not propose a temperature difference at which the energy balance estimation is accurate.

Thus, it is purposed to study the range of temperatures at which the OA ratio estimation is valid compared to a physical flow meter. We can correlate the OA ratio to the damper position using that information instead of the OA flow rate. Using the OA ratio will reduce the error associated

with pressure variation due to its similar influence on supply and outdoor flow. Moreover, a supply VFM will be implemented for OA flow measurements.

Overall, it is assumed that using the energy balance equation to model a correlation to the damper position is better than using it to dynamically measure the OA ratio because the VFM will not have limitations associated with relative temperature values.

This thesis will answer the following question regarding VFM for chiller water flow rate and outdoor airflow rate.

Chilled water virtual flow meter:

-How does chilled water VFM perform under high (Summer) and low conditions (Winter)?

-Does the integration of cascade control perform well under high and low conditions (no need for gain resets)?

-Can cascade control help stabilize supply air temperature under Dp changes?

Outdoor air virtual flow meter:

What minimum value of (TRA - TOA) is required to obtain accurate OA ratio reading using the energy balance equation?

- Can we correlate the OA ratio to the damper position?

-What is the influence of mixing chamber pressure on such a correlation, and can it be eliminated?

Chapter 3 : Methodology

3.1 Experimental and Mathematical Models

Before experimental testing, the VFM was developed based on specific models proven to provide positive results, as shown by Song *et al.* and Wang *et al.* These models are important to re-create the behavior of AHU components such as the CHW valve and outdoor air flow sensor. The models utilize the building automation system inputs to compute the target output value. The inputs were used to regress the empirical characteristics of the tested equipment. On the other side, thermal properties of temperature inputs used an energy balance relationship to compute the target results.

3.1.1 CHW-VFM

The development of CHW-VFM is based on two steps; the first is to model the valve behavior and correlate it with the chilled water flow rate; the second is to integrate a cascade control model to enhance the VFM performance.

The following model was developed and proposed by Song et al. and Swamy *et al*. with a confidence of 99% compared to using an ultra-sonic meter. The model relies on using the inherent flow characteristic of the operating valve. These characteristics define the relationship between the valve opening percentage and the chilled water through it under constant external conditions such as differential pressure [19]. It is crucial to note that these characteristics are based on empirical coefficients obtained upon installation.

Chilled water valves are responsible for regulating chilled water flow across the cooling coil based on cooling load requirements. As discussed in Chapter 2, a chilled water pump is responsible for maintaining a constant DP within the chiller water loop to satisfy the needs of

different cooling coils sharing one network. Thus, the chilled water valve modeling and its correlation to the cooling coil depend on the valve's differential pressure readings (ΔP_V).

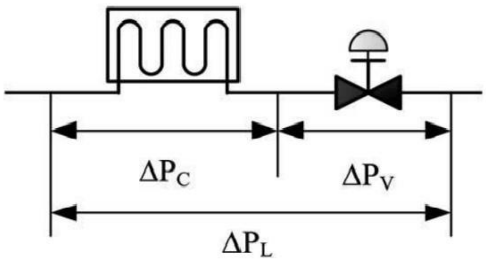


Figure 3-1 Layout of CHW valve and cooling coil and their corresponding DP [19]

The differential pressure sensor is installed across the cooling coil and valve in the testing layout used, as shown in Figure 3-1. Therefore, the reading obtained during the testing is ΔP_L. However, to model the valve behavior based on ΔP_V, Swamy *et al.* proposed using the valve authority (N) that correlates the ratio between ΔP_V and ΔP_L using the following equation [19]:

$$N = \frac{\Delta P_{v,d}}{\Delta P_{L,d}} \quad \text{Equation 1}$$

Where

N = The valve authority.

$\Delta P_{v,d}$ = differential pressure across the valve.

$\Delta P_{L,d}$ = differential pressure across the (cooling coil + valve).

Consequently, the pressure across the valve is defined using this equation:

$$\Delta P_{v,d} = \Delta P_{L,d} - \Delta P_{c,d} \quad \text{Equation 2}$$

Where

$\Delta P_{c,d}$ = differential pressure across the cooling coil.

He also added that the DP across the cooling coil for an open valve position is proportional to the product of the water flow ratio squared and the cooling coil DP under design conditions. The water flow rate ratio is defined as:

$$\bar{Q}_x = \frac{Q_x}{Q_d}$$ Equation 3

Where

Q_x = the volumetric water flow rate under any valve position x.

Q_d = the volumetric water flow rate under design conditions.

Overall, the DP across the valve for a specific valve position x can be defined as follows:

$$\Delta P_{v,x} = \Delta P_{L,x} - \bar{Q}_x^2 \,.\, \Delta P_{c,d}$$ Equation 4

Where

$\Delta P_{L,x}$ = the differential pressure across the (cooling coil + valve) for valve position x operation.

Moreover, the valve resistance coefficient ($K_{v,x}$) for a specific valve position x is defined as:

$$K_{v,x} = \frac{\Delta P_{v,d}}{(R^{x-1})^2} = \frac{\Delta P_{v,d}}{\bar{Q}_x^2}$$ Equation 5

Where

R = valve rangeability

If the valve is fully open, then x = 1.

If the valve is fully closed, then x = 0.

The valve flow coefficient (C_v) is defined as:

$$C_v = \frac{Q_d}{\sqrt{\Delta P_{vd}}}$$ Equation 6

Altogether, the water flow rate can estimate using valve properties and differential pressure across (cooling coil + valve) using the following relation:

$$Q_x = F_{L,x}(x)\sqrt{\Delta P_{L,x}}$$ Equation 7

$F_{L,x}$ (x) is defined as the valve characteristic curve [11].

$$F_{L,x}(x) = \sqrt{(C_v \,.\, (R^{x-1}))^2 \; N/[N + (R^{x-1})^2(1-N)]}$$ Equation 8

When experimentally validating CHW-VFM by Song *et al.*, the valve position x was obtained using the valve command signal from the building automation system. Instead, this study will use the valve feedback signal to eliminate any inaccurate readings caused by the valve time constant. In addition, using the feedback signal will help obtain accurate real-time flow readings.

3.1.2 Cascade Control

The integration of cascade control will follow the layout shown in Figure 3-2, where "A" is the outer loop and "B" is the inner loop. The outer loop consisted of a traditional PI loop with the supply air temperature setpoint "1" as its reference input, the supply air temperature measurement "4" as its input values, and the chiller water flowrate setpoint "2" as its output.

The second loop will consist of a P controller with the chiller flowrate setpoint "2" as its reference input, the chiller water flowrate measurement as its input value “5”, and the CHW-valve position "3" as its output.

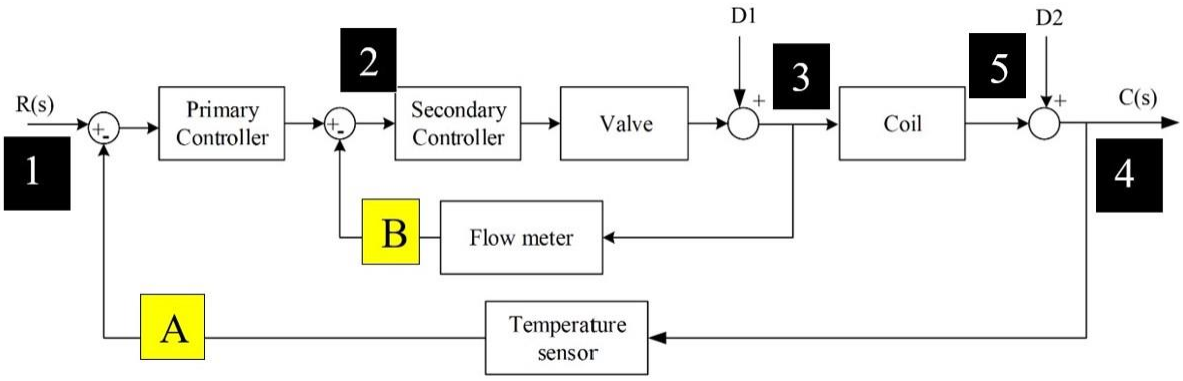


Figure 3-2 The layout of the proposed cascade control

Proportional and proportional-integral controllers for the inner and the outer loop are based on the cascade control model proposed by Elliott *et al*, which suggests using a fast inner loop and slow outer loop [34]. A faster inner controller is due to the higher gains associated with the cooling coil, which requires a quicker response to stabilize the dynamic changes.

As cascade control performance is compared to a traditional single control, the following model was used for the single control testing.

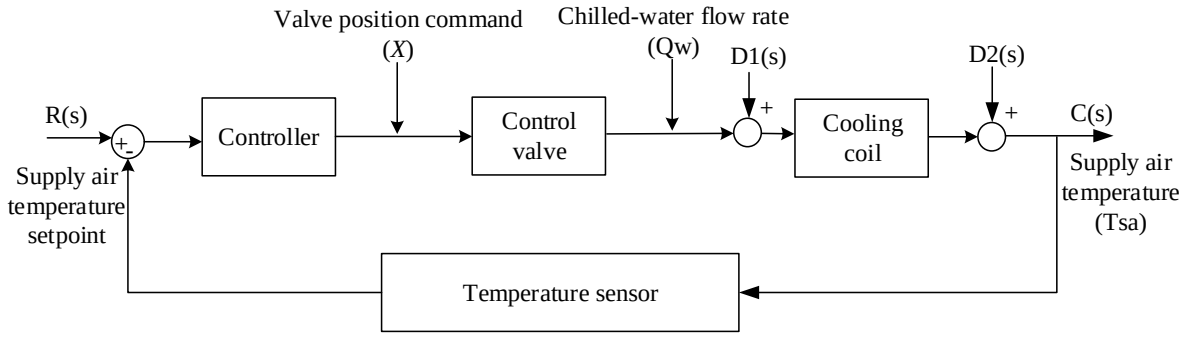


Figure 3-3 Layout of single control model used for cascade comparison study

3.1.3 OA-VFM

The development of outdoor air VFM relied on estimating the outdoor air ratio (α) at certain outdoor air damper position (ϑ) according to the following energy balance equation using a set of operational data under favorable operations when the errors presented by the temperature measurements have minimum impact:

$$\alpha(\vartheta) = \frac{T_{MA} - T_{RA}}{T_{OA} - T_{RA}} \quad \text{Equation 9}$$

Where

T_{MA} = Mix air temperature

T_{RA} = Return air temperature

T_{OA} = Outdoor air temperature

ϑ = Outside air damper position

The collected data will be used to regress the correlation between the outdoor air ratio and damper position, shown in Equation 10. The outdoor air ratio can then be calculated using the regressed correlation without the energy balance calculation.

$$\alpha = function(\vartheta) \quad \text{Equation 10}$$

If outdoor airflow measurement is required over the outdoor air ratio value, then Equation 9 can be used in addition to Equation 11 to compute that value.

$$Q_{OA} = \alpha \times Q_{SA} \quad \text{Equation 11}$$

Where

Q_{OA} = Outdoor airflow rate

α = Outdoor air ratio

Q_{SA} = Supply airflow rate

The development of outdoor air VFM will follow these steps:

1) Data collection
2) Outdoor air ratio estimation using Equation 9
3) Estimation vs. measurement comparison
4) Correlate outdoor air ratio with damper position

3.2 Test Design

Four tests are designed to validate the modeling methods introduced in Section 3.1. They are presented according to the order of models. Each test will include the testing conditions, parameters and step changes conducted. Its important to note that all non-measured variables were maintained at steady state for control purposes.

Test 1: Chilled Water Valve

Test 1 conditions were used to correlate the valve position and flow rate to retrieve the valve characteristics. The chiller water loop DP is controlled by a building tertiary pump that uses VFD to maintain a stable DP set point of 17 PSI across all the shared cooling coils. Thus, it is crucial to monitor the DP stability to avoid flowrate instability associated with DP fluctuations. Also, the outdoor air damper was set to 0% to reduce any external influences on the cooling loads that may disturb the system's performance during the test.

The test consists of manually overridden valve commands ranging from 0% to 100% with a 5% step change. The 0%-100% range was performed in ascending and a deceasing order to investigate any possible hysteresis behavior associated with the valve operation. The step time associated with each incremental change is 10 minutes; thus, the total test time of 6 hours and 40 minutes.

Test 2: Cascade Control Integration

This test is used to investigate the performance of cascade control plus CHW-VFM under different operating ranges compared to a single controller. A set of test cases are designed and performed under two cooling load conditions, a low load and a high load condition.

Based on the model presented in Figure 3-2, the WorkPlace VISIO software was used to construct the cascade control and integrate the CHW-VFM in its operation, shown in Figure 3-4. The CHW-VFM was used in the inner loop to perform flow rate measurements for the secondary controller input "3". However, the software has constraints associated with the type of operations it can achieve. Thus, to input the valve characteristics curve found in Equation 8, the curve was built using pre-determined linear segments that match the resulting curve. Also, the PID output in the software is a percentage value for actuation purposes. Therefore, the water flow rate was interpolated based on the design water flow rate of 9.5 GPM, with 0% equating to 0 GPM and 100% equating to 9.5gpm.

Shown in Figure 3-4, area B, a valve position feedback signal from the BAS was used as an input to compute the resistance coefficients dynamically. Coefficients are then multiplied by the square root of the DP signal to calculate the real-time chilled water flow rate virtually.

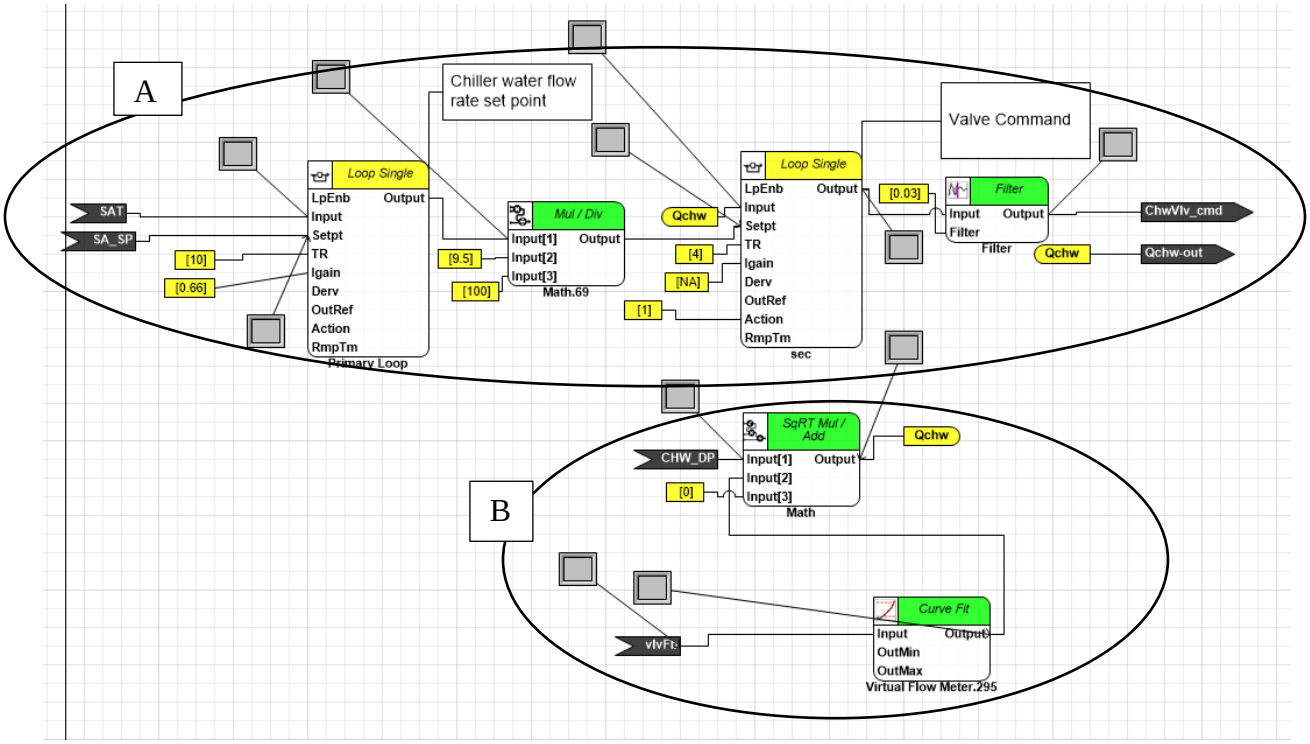


Figure 3-4 Operation template of the CHW-VFM "B" integrated into the cascade control "A"

The investigation includes 8 test cases that aim to test the CHW-valve cascade control performance under two system disturbances. The first disturbance is a step-change reference input in the supply air setpoint, which causes a sudden change in the CHW flow rate. The second disturbance includes a step change of DP in the chilled water loop. The DP sudden change will result in cooling coil gain changes as its directly impacted by the DP gains. As a result, we can investigate the stability of the CHW-VFM that is based on design gain values and the inner loop's performance. As mentioned, both disturbances are evaluated under high and load system conditions.

Moreover, the test conditions were also evaluated for a traditional single controller to allow for a comparative study of the performance of cascade and single controllers. The PI/P controller settings were the same during all tests. The controller settings are tuned to design conditions

(high load) for both single and cascade control. Using design conditions, we can investigate the performance under low conditions that usually require seasonal gain resets due to instability. Hurt *et al.* studied the difference between cascade control and a single controller that isn't accurately tuned. Thus, his findings showed the performance difference based on generic controller properties [25]. By accurately tuning both controllers, we can show the superiority of cascade control even when a single controller is tuned accurately.

Table 3-1 Details of the test cases performed for the cascade control study

Test Case	System Condition	Supply airflow (CFM)	Controller Type	Outside air ratio	Step change Type	Step change value
Case A	Low	1000	Single	0	Supply air temperature	55F° to 57F°
Case B	Low	1000	Cascade	0	Supply air temperature	55F° to 57F°
Case C	Low	1000	Single	0	Differential Pressure	17Psi to 10Psi
Case D	Low	1000	Cascade	0	Differential Pressure	17Psi to 10Psi
Case E	High	1800	Single	0	Supply air temperature	55F° to 57F°
Case F	High	1800	Cascade	0	Supply air temperature	55F° to 57F°
Case G	High	1800	Single	0	Differential Pressure	17Psi to 10Psi
Case H	High	1800	Cascade	0	Differential Pressure	17Psi to 10Psi

The supply flow rate was maintained at 1000 CFM for low and 1800 CFM for high load conditions to simulate the required cooling load conditions. The terminal boxes' airflow setpoints were changed to maintain the supply flow rate until their total setpoints matched the required supply airflow rate. Other methods of overriding supply airflow rate are to control the VRF of

the supply fan. However, the terminal box's dampers actuate as a function of duct pressure; when the supply fan is overridden, the system will maintain a constant TB damper position. Consequently, variations in the supply fan speed can cause pressure changes in the duct and the building.

Each test case had a run time of 20 min and was recorded using the HOBO loggers measuring at a 1-second interval. The HOBO loggers recorded $T_{SA,}$ T_{MA}, DP, $Q_{SA,}$ CHW-valve command, and CHW-valve feedback. In addition, supply air temperature and DP step changes were performed in the VYKON N4 building automation system.

Test 3: Outdoor Air Measurements

The following test is performed to collect outdoor air ratio estimation data using Equation 9. To understand the system's behavior and its effect on OA estimation, variables recorded are mixed air, return air, outdoor air temperature, outside air damper command and feedback, and supply and outdoor airflow rates. The test was run for a period of one week and one month. The two periods help us determine the sample size necessary to implement an accurate VFM. Also, the test was implemented during a period of a large variation in temperature to be able to study a large range of temperature differences ($T_{RA} - T_{OA}$). No additional system overrides were used in this test. The time and data were stored and obtained from the building automation system at a 1-minute sampling rate.

Test 4: Outdoor Air Damper Correlation

The outdoor air ratio estimation as a function of outdoor air damper position is sensitive to pressure variation [35]. Therefore, Test 4 aims to study the effect of mixing chamber pressure changes on the outdoor air ratio as a function of damper position. Pressure changes are induced

by the supply and return fan speed, especially for systems using offset tracking methods [29]. We can maintain constant chamber pressure by maintaining a fixed system airflow rate. Doing so will allow us to study the OA ratio vs. damper position correlation. The outdoor ratio estimation will also be studied under different systems flow rates to show the effect of chamber pressure on OA ratio measurements as a function of damper position.

Using a ramp function, the outdoor air damper position from 5% to 50% with a 5% step change every 20 minutes. The total run time of damper position changes was 160 minutes. The outdoor air damper positions were repeated for a different supply airflow rate ranging from 800CFM to 1800CFM with a 200CFM step-change induced at the end of the 160 minutes. No additional system overrides were used in the test.

The system's airflow rate was controlled using the TB airflow setpoint as was done in test 2 to avoid building pressure changes that can influence the mixing chamber pressure under different fan speeds

3.4 Testing Layout

This thesis is an experimental study to test and validate VFM on an AHU during operating conditions. Thus, a commercial AHU was used for all testing. Before introducing the testing layout, understanding the relevant components is required.

3.4.1 Operational Background

Figure 3-5 shows a basic layout of the air handling unit. The unit primarily consists of intake dampers (Outside air and return air), a cooling and heating coil for air conditioning purposes, and fans (supply and return) used to move and circulate air around thermal spaces (externally) and

the system (internally). The nature of the experimental work focuses on the operation of both the chilled water coil (1) and the outdoor air intake (2), as shown in Figure 3-5.

A space is traditionally maintained in a range of temperature and humidity conditions specified by ASHRAE standard 55 to meet thermal comfort [36]. For a typical space, 75 F° and 55% relative humidity are used to achieve ASHRAE standard 90.1. To meet these space conditions, a supply air temperature of 55 F° is required to balance out both sensible and latent heat gains. Consequently, an AHU's primary function is to provide a stable 55 F° stream of air to the conditioned rooms.

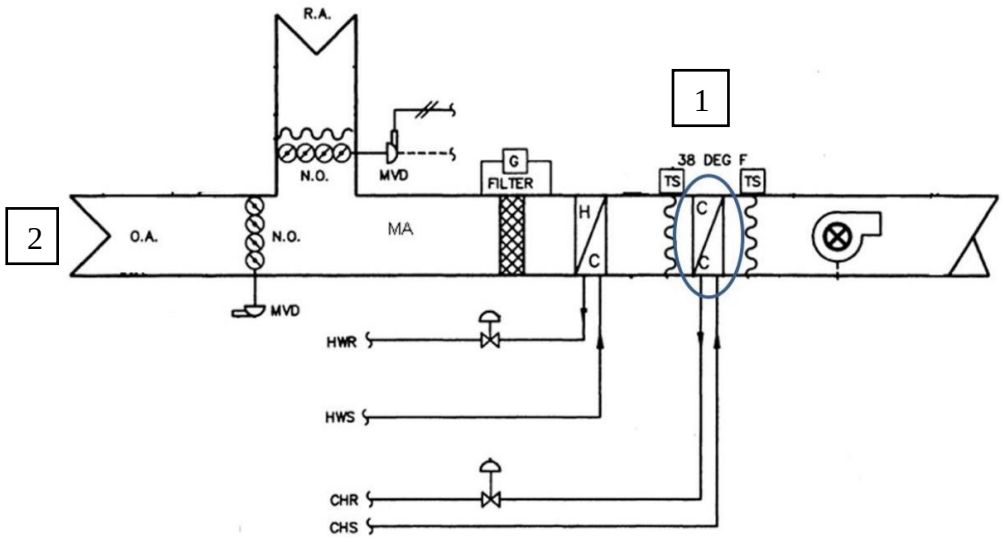


Figure 3-5 Basic layout of traditional AHU

As a result, air undergoes conditioning through the cooling coil. A cooling coil is a traditional heat exchanger consisting of tubes to circulate chilled water or cooling refrigerant across metal fins used to absorb sensible and latent heat from the mixed air until the air reaches 55 F°.

$$Q = 500 \times \text{GPM} \times \Delta T \qquad \text{Equation 12}$$

The cooling coil effect on passing air is quantified using the thermodynamic relation above. Q is the heat transfer rate, GPM is the chilled water flow rate measured in gallons per minute, and delta T is the water temperature change across the coil. Typically, a cooling coil uses chilled water supplied at a fixed temperature by a central chiller plant. As a result, Equation 12 states that the flow of cooling matter is proportional to the change in temperature.

It is important to note the relevance of cooling coil operation to the stability of supply air temperature as instant air temperature changes require fast flow rate adaption to maintain a stable 55 F° supply air temperature. Also, fluctuations in supply air temperature cause variations in the chilled water pump flow rate, increasing operational cost and lowering pump efficiency [26].

The outdoor air operation is regulated by air dampers using actuating signals from the BAS. This operation is crucial to ensure proper ventilation (CO_2 levels) according to ASHARE 62.1. The significance of outdoor air operations is crucial for ventilation purposes and to ensure a low-cost operation. As mixed air properties -temperature and relative humidity- are different from the supply air condition, a higher conditioning load is required, thus leading to higher operating costs. Consequently, minimum outdoor air intake is maintained during hot seasons to minimize cooling loads while maintaining ASHRAE 62.1 standards for ventilation rates.

Moreover, to understand some findings of this thesis, it is important to discuss the relationship between the system's operation and building pressure.

Building pressure is maintained using the AHU fans. Positive building pressure is usually maintained to avoid air infiltration due to door openings or structural cavities. Outdoor infiltration is undesired to keep contaminant, dust, and unconditioned air outside the building [37]. It is controlled by maintaining a flow rate difference between the supplied air and the return

air. However, due to the lack of a flow sensor in common AHU, an offset tracking method is used to maintain a fixed speed difference between the supply and return fan; it is deemed unreliable due to the different fan curves associated with each fan [29].

3.4.2 Test Bed

The AHU used for this study is a single duct VAV -utilizes VFD fans- unit with 8 tons cooling capacity. The unit serves seven thermal zones -seven terminal boxes- equipped with reheat coils for heating operation. It is located in the engineering lab (EL) building at the University of Oklahoma in Norman, Oklahoma. The AHU uses chilled water for its cooling coil supplied from a central chiller plant at the University of Oklahoma, serving other AHUs across the university.

The building (EL) air conditioning does not only rely on this AHU, but a second larger AHU is shared to meet the building loads. This study has no operational control over the second AHU. Therefore, the nature of the open space (no sectional separation) can cause instability in the experimental unit due to the operation of the other AHU, especially during tests involving building pressure and temperature control.



Figure 3-6 The AHU used for the experimental study.

The system consists of the same components shown in Figure 3-5. In addition, the system includes sensors measuring the supply and return fan drive information (Hz, power, and voltage); mix-air, supply, pre-heat, return, and outdoor air temperatures; supply and outdoor airflow rate. On a chiller loop level, sensors measuring DP, chilled water temperatures, and flow rate across the cooling coil are installed along with a chiller water valve command and a feedback signal.

Installed in place is a TUF-2000M ultrasonic meter used to measure chilled water flow across the cooling coil. This meter is used for its non-invasive installation compared to the differential pressure and traditional velocity meters. An ultrasonic meter operates through propagating ultrasonic waves between two transducers installed in place to calculate the velocity of the traveling medium (chilled water). The velocity is then multiplied by a pre-set value of the cross-sectional area of the container (pipe) to determine the flow rate.

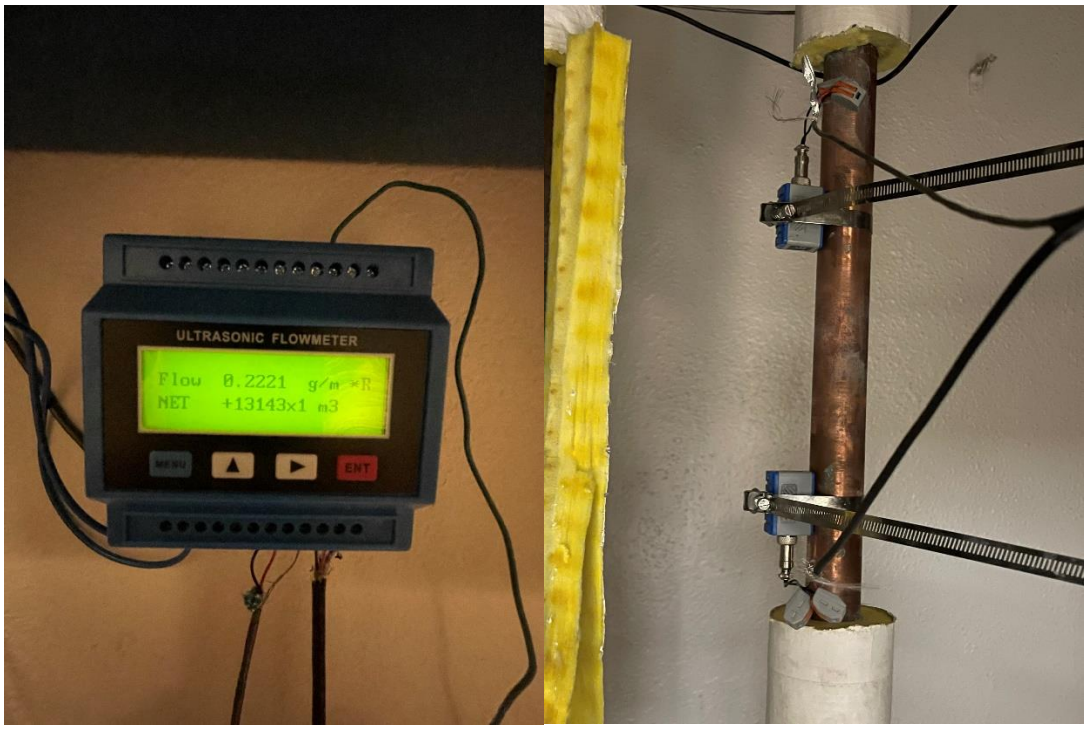


Figure 3-7 The Ultrasonic meter used for CHW flow a) Module b) Transducers mounted on the CHW intake pipe

According to the module manual, this sensor has an accuracy of 1%. However, this accuracy is dependent on the alignment and spacing of both transducers upon installation. In addition, the meter requires ultrasound gel that acts as a conducting medium between the transducers and the measured medium. Therefore, maintenance every 3-4 months is required to replace the gel and restore reading accuracy.

Altogether, such a meter is prone to low accuracy due to human errors during installation, which can reduce potential cost savings due to inaccurate readings. In addition, aside from the initial installation cost, this meter comes with periodic maintenance costs.

The flow of outdoor air is measured using a duct traverse. It consists of 3 velocity probes evenly spaced through a cross-sectional area of the outdoor intake straight duct. Velocity readings from all probes are averaged to reduce the effect of air turbulence and account for velocity profiles across the duct. The averaged velocity measured in feet per minute (fpm) is multiplied by the duct area to retrieve the flow rate in cubic feet per minute (CFM). Moreover, the velocity probe consists of a hot-wire anemometer that uses a hot wire heated to a constant value. As air flows through the heated wire, heat dissipation is created between the air and the wire affecting its resistance. The change in resistance is correlated to the flow rate. However, measurements can be affected by the temperature drifts in the heated elements because of changing ambient temperatures, creating larger measuring errors under high-temperature drifts.

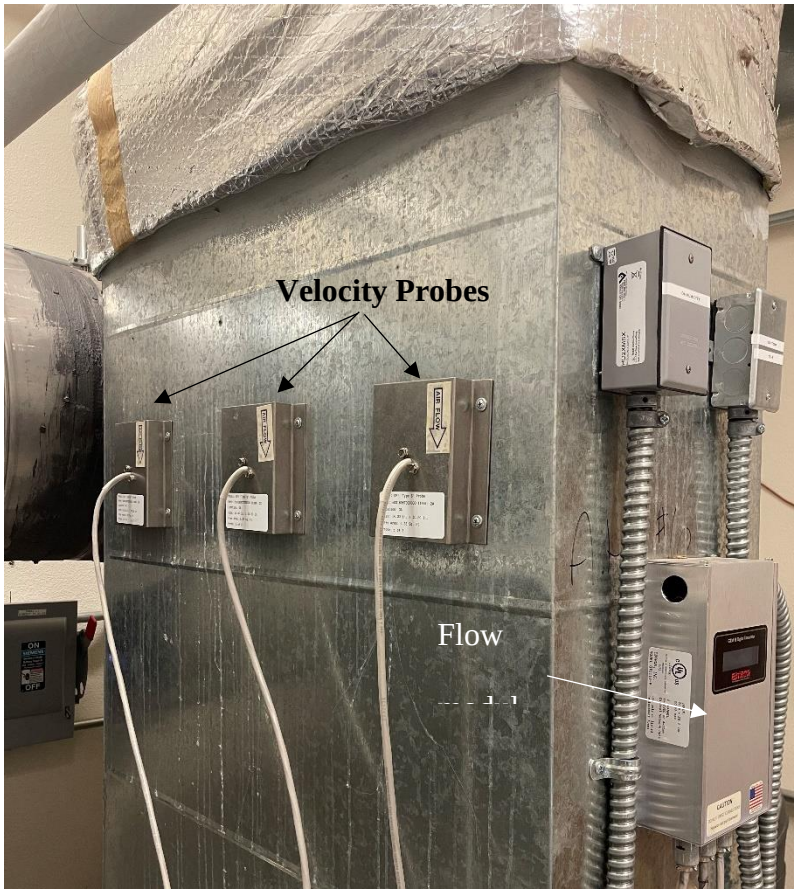


Figure 3-8 Duct Traverse performed for outdoor airflow measurements

To develop the CHW-VFM for the AHU used, the AHU's valve characteristics curve needs to be obtained. An empirical approach was used as proposed by Song *et al.* in which water flow and DP measurements are collected from the BAS using physical meters -mentioned in 3.2.



Figure 3-9 The chilled water valve used in the experiment

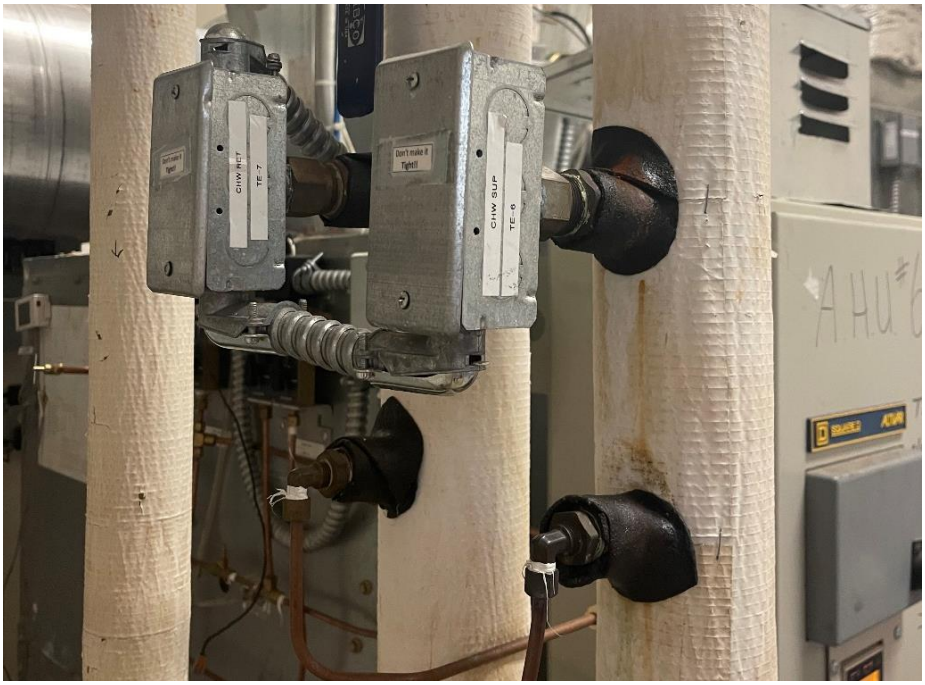


Figure 3-10 Differential pressure sensors installed to measure ΔP_L

The system uses a building automation system (BAS) operated by several Schneider MNL-800 controllers that collect data from all sensors and perform actions using a pre-set algorithm to control the AHU and the individual VAVs for each thermal zone. Controllers are communicated

using "VYKON Workplace N4" software, presented in Figure 3-11. The software can read and write to and from the controllers to perform overrides and test operating algorithms for research purposes across the total system (AHU, VAVs, chiller water loop). All values are collected and archived with a 1 min sampling rate inside the software and can be viewed and exported for further analysis.

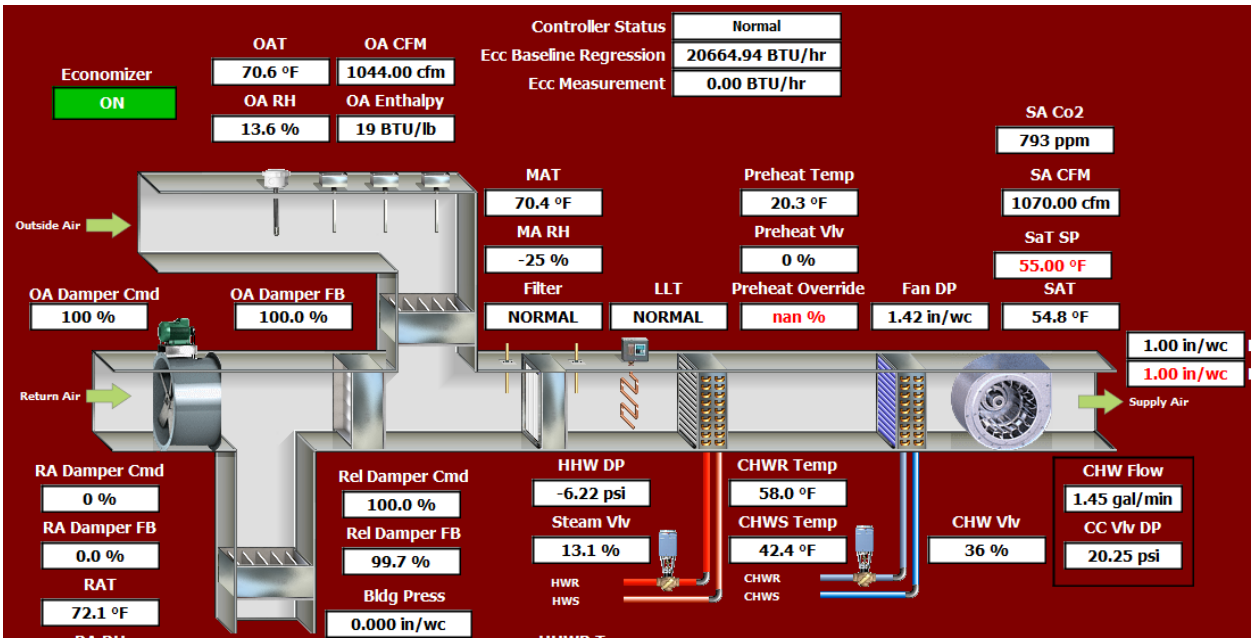


Figure 3-11 An overview of the VYKON N4 readings recorded by the system's controller.

However, certain testing conditions require a higher resolution (< 1 minute) to understand the results accurately. Therefore, a set of HOBO 4-channel analog data loggers are installed to duplicate measurements done in the BAS. The loggers can measure and store values with a 1-second sampling rate.

The loggers included measurements of supply, return, mix air temperatures, CHW-valve command and feedback, and supply and return fan operating conditions (DP, Hz, power, and flow rates).

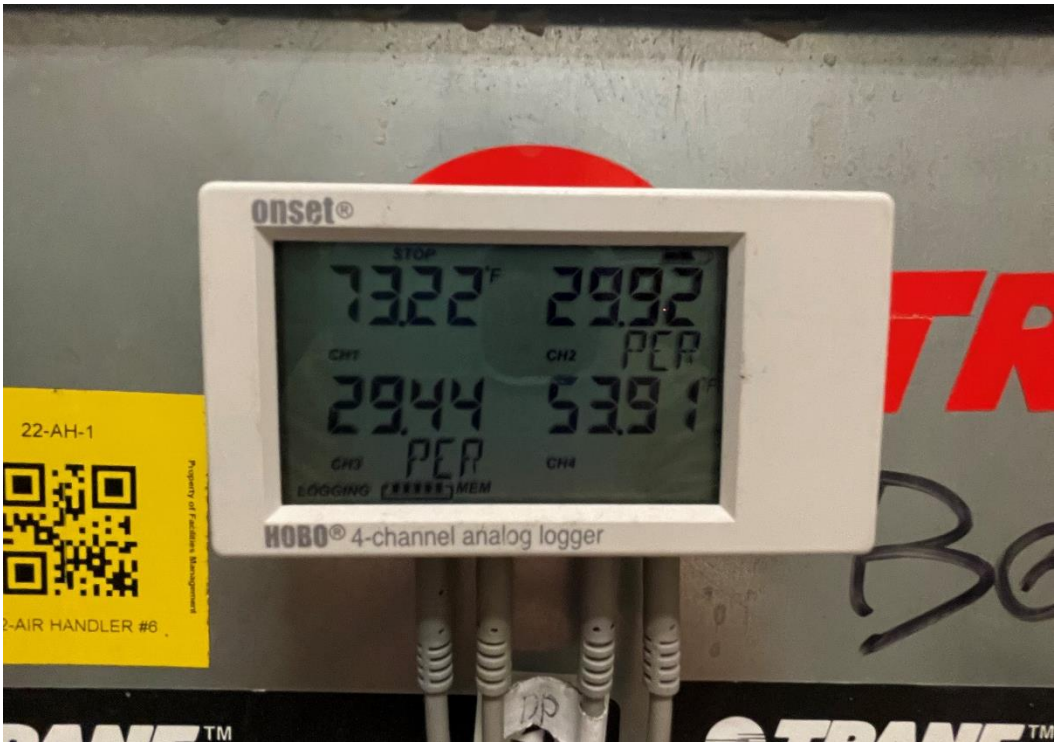


Figure 3-12 HOBO data logger installed to measure T_{MA}, CHW-valve command, CHW-valve feedback, and T_{SA}

Chapter 4 : Results and discussion

Presented are the results of the tests cases performed in Chapter 3.

4.1 CHW-VFM Performance Analysis

For the implementation of the VFM, the valve characteristics curve was determined using Test 1. Figure 4-1 shows the difference between the valve command and feedback signal where no significant difference in the signals is observed. The error between the command and feedback signal is less than 5% overall. However, we notice that the valve experiences a dead band when the command signal is larger than 95%, as shown in Figure 4-3. A dead band occurs when the command signal results in no feedback change, thus a constant output [38].

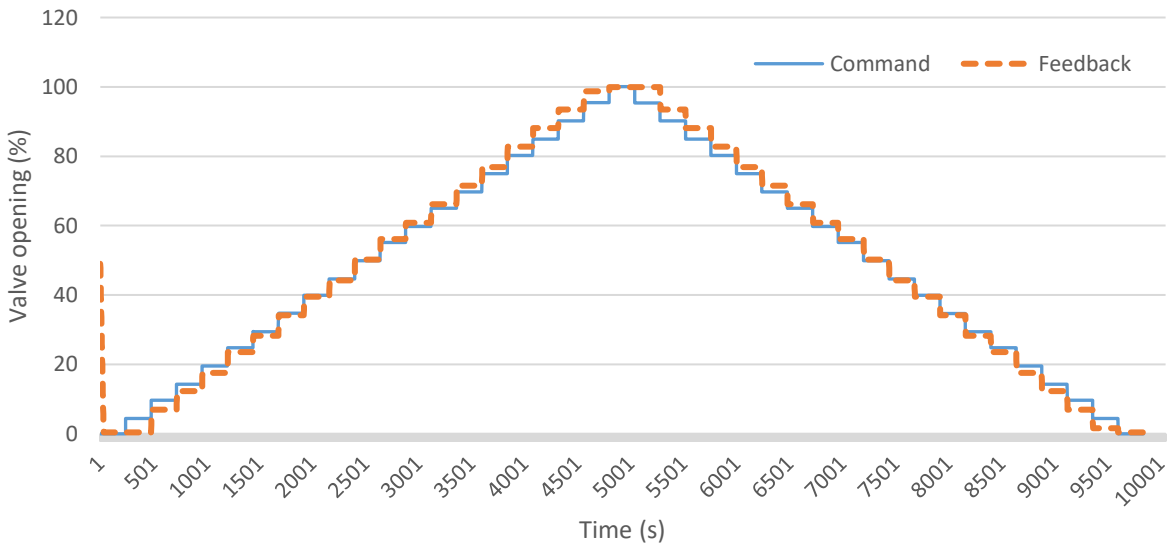


Figure 4-1 Valve command and feedback signal of valve position step changes performed

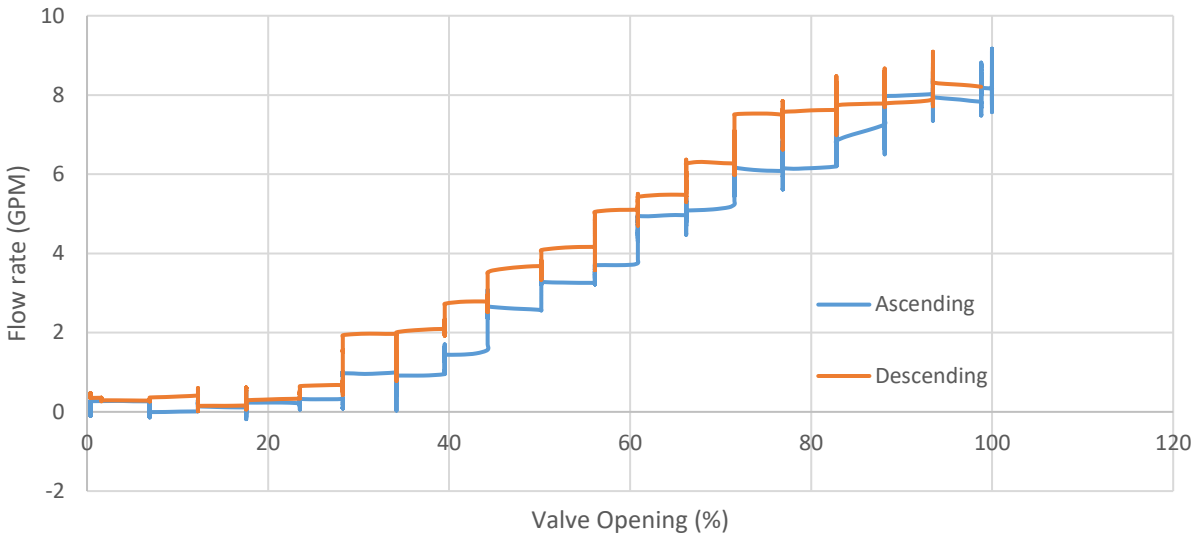


Figure 4-2 Chilled water flow rate vs. valve opening % measured using the ultrasonic meter

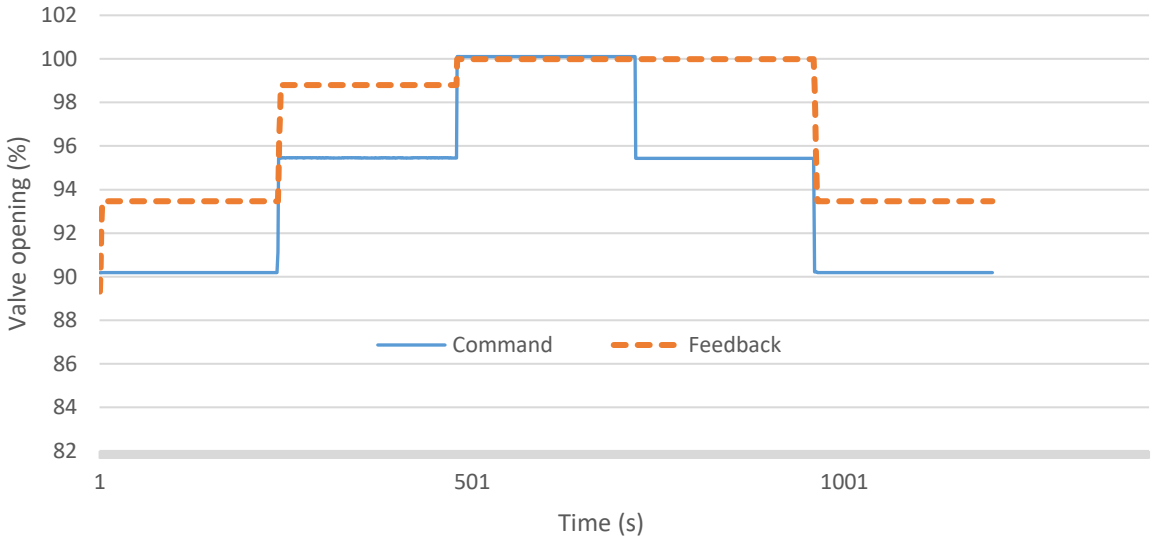


Figure 4-3 Valve dead-band experience at command signals larger than 95%

The chilled water flow rate measured in GPM depends on the valve position, shown in Figure 4-2. When the valve is experiencing a dead band at 95% valve position, the resultant flow rate is constant, with an average flow of 8.235 GPM. Due to the range of valve positions covered

during the test's operating conditions, the dead band will be disregarded as it is outside the relevant range of operation.

In addition, the valve experienced nonlinearities due to the different valve position gains. At a lower range of valve positions (< 30%), we can see that the small gain results in a small to no change in chilled water flow rate. However, the same small gain is experienced at valve positions larger than 80%. Figure 4-4 shows the nonlinearities associated with the variation of valve gain at different positions.

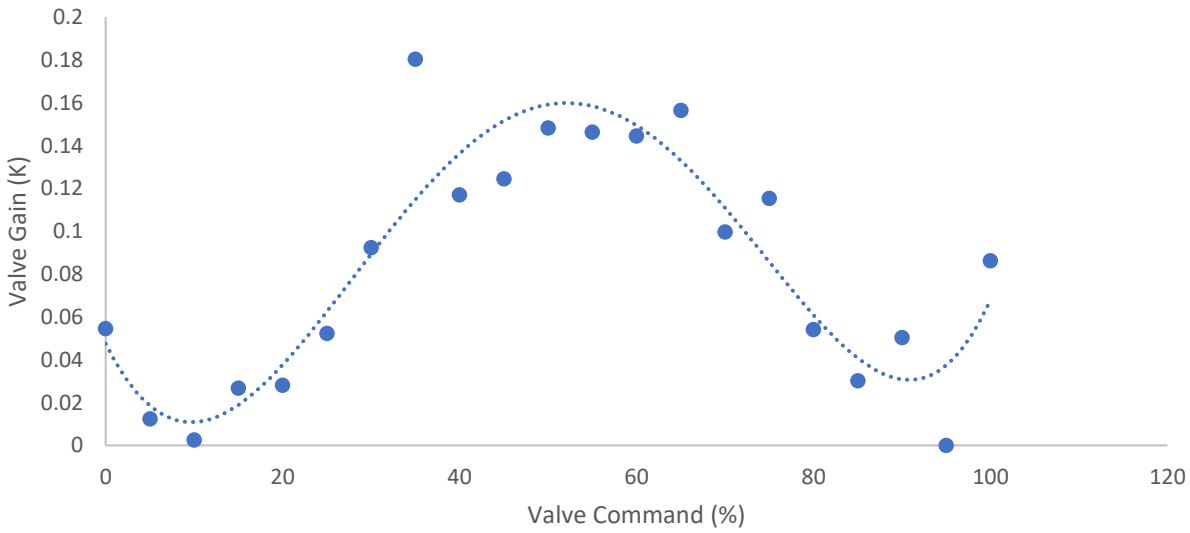


Figure 4-4 Valve gain (K_v) associated with each valve position

Also, Figure 4-2 suggests valve hysteresis, where the chilled water flow rate is relatively higher in the descending order than in the ascending. Such hysteresis can be attributed to a higher DP measurement in descending direction. A higher DP results in an increased valve gain, thus, a larger flow rate. Also, the range of chilled water flow variation per fixed valve position coincides between the ascending and descending order; thus hysteresis effect can be reduced by taking the average of the total flow readings per a fixed valve position.

As mentioned in Chapter 3, it is important to maintain a stable DP value as it directly impacts the valve gain. Therefore, maintaining a stable DP value will eliminate valve gain changes due to DP and will be mainly impacted by the chilled water flow rate across the valve. Throughout the test period, DP was maintained at an average of 18.08 PSI. However, this average was obtained from the fluctuation range of 16.4 – 19.5 PSI. These fluctuations result from the tertiary pump behavior, which experiences oscillatory flow due to the pump's mechanical operation. In addition, other flow variations can be caused by load changes as the tertiary pump is shared between two AHUs. Overall, the resulted fluctuations were consistent throughout the test.

The average flow and DP value were computed, and using Equation 6, the valve flow coefficients C_v were computed for each valve position. Plotting the C_v against the valve position will result in the valve characteristics curve. Using trendline regression, a polynomial to the fifth-order was used to regress the resulting curve shown in Figure 4-5.

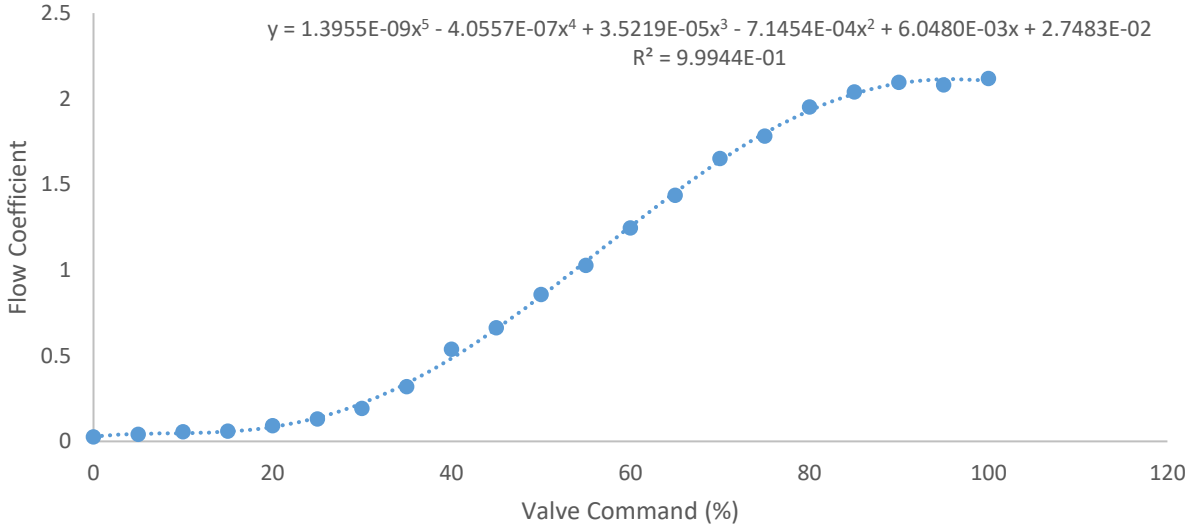


Figure 4-5 Valve flow coefficient (C_v) vs. the valve command signal.

Therefore, the valve characteristic curve is:

$$F_{L,x}(x) = (1.395 \times 10^{-9})x^5 - (4.055 \times 10^{-7})x^4 + (3.522 \times 10^{-5})x^3 - (7.145 \times 10^{-4})x^2 + (6.048 \times 10^{-3})x + 2.748 \quad \text{Equation 1}$$

Using Equation 7 and Equation 13, we can measure chilled water flow rate virtually as a function of valve position (x) and DP measurement. This CHW-VFM is unique to the used valve based on empirical values obtained from test 1. As mentioned in Chapter 3, to model this characteristic in the HVAC controller (Schneider MNL-800), we need to input linear segments that match the resulting curve. Therefore, four segments were determined, as shown in Figure 4-6.

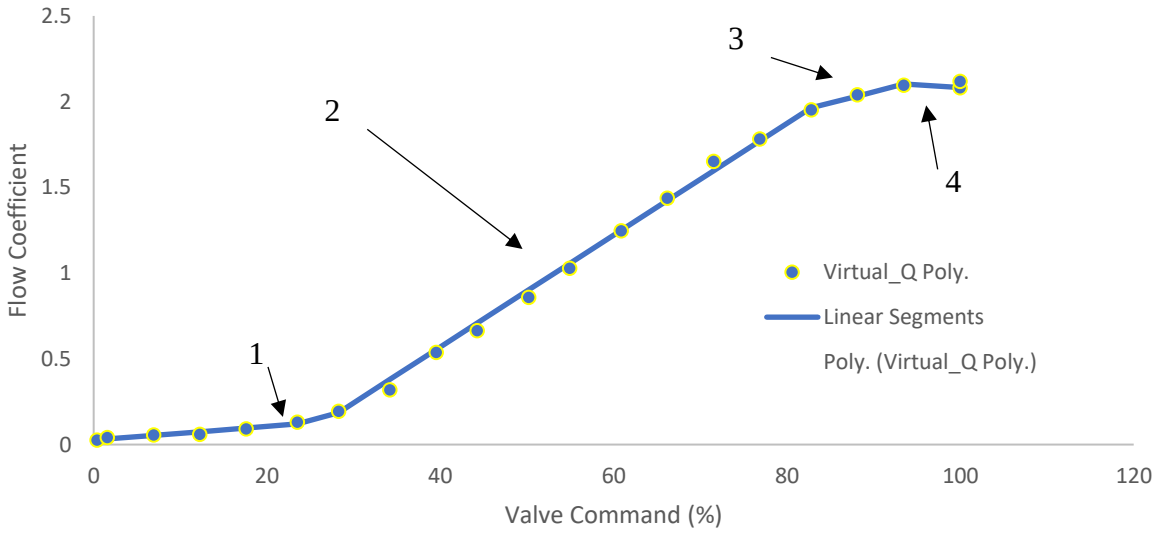


Figure 4-6 Valve characteristics curve divided into four linear segments

The resulting equation and range for each linear segment are included in Table 4-1.

Table 4-1 Equations of characteristics curve linear segments and their operating range

Linear segment no.	Equation f(x)	Range (x)
1	$0.004x + 0.026$	$0 \leq X < 25$
2	$0.033x - 0.734$	$25 \leq X < 80$
3	$0.014x - 0.841$	$80 \leq X < 90$
4	$-0.002x - 2.321$	$90 \leq X < 100$

After implementing the VFM in the AHU's controller, as shown in Figure (3-4. B), the meter was tested for different valve opening with a 5% step change as performed in the test. Figure 4-7 shows the chilled water flow rate measured from the ultrasonic meter and the VFM. It also includes the standard deviation of the VFM. The standard deviation of the VFM was less than that of the ultrasonic for valve positions, less than 80%. This shows that the ultrasonic meter is prone to noise affecting its reading accuracy, unlike the VFM. However, for valve positions larger than 80%, the VFM STD was higher than those of the ultrasonic, attributed to the valve's dead band, non-steady gains, and low valve resolution experienced at that range. Overall, the mean relative error of the VFM is less than 5% which gives high reliability to replacing the physical flow meter with the VFM.

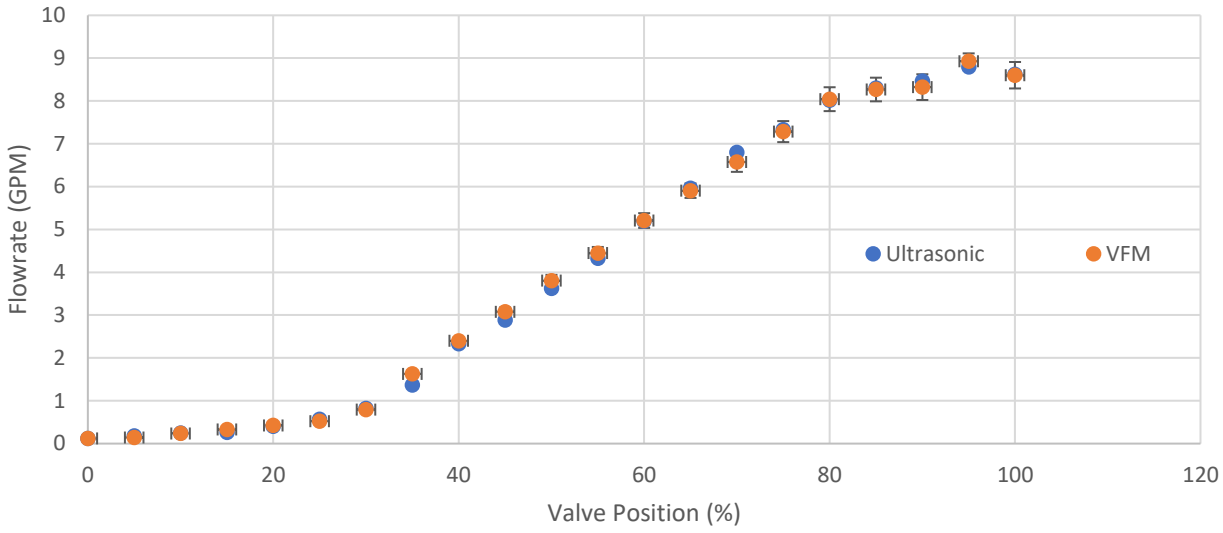


Figure 4-7 Chilled water flowrate measured by the ultrasonic meter and the built VFM with STD values

As discussed in Chapter 2, sensor errors can result in higher operational costs. Figure 4-8 shows the error associated with the physical flow meter (ultrasonic) when reaching its maintenance due time (3 months). The ultrasonic had an average error larger than 100% compared to its calibrated condition. Therefore, using a VFM will eliminate this error and the need to perform periodic maintenance, which results in additional costs.

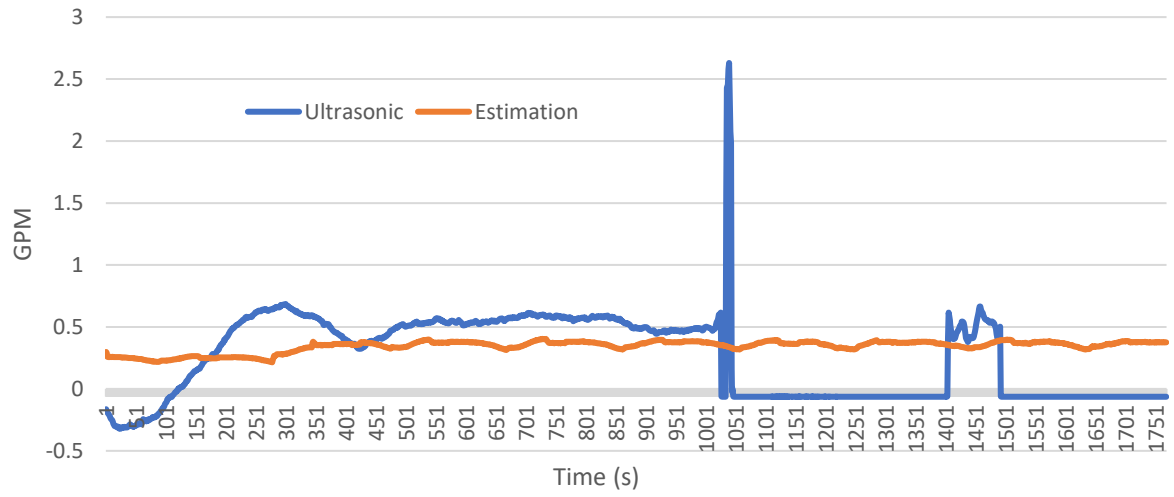


Figure 4-8 Chilled water flow measurement using VFM and ultrasonic meter nearing its maintenance due time.

4.2 Cascade Control Performance Analysis

The CHW-VFM was used in the cascade control inner loop controller to compute chilled water flowrate. After uploading the cascade control layout shown in Figure 3-4, test (2) with its 8 cases was conducted, and the results were as follows.

4.2.1 Operation under Low Load Condition

For cases A and B performed with step change of supply air temperature set point from 55 to 57, Figure 4-9 shows the controller performance based on its reference input (supply air setpoint) and the chilled water flow rate response. Both accurately tuned controllers reached the T_{SA} set point in less than 3 minutes. Therefore, if a single controller is tuned precisely, a faster performance can be achieved than a slower controller -used by Hurt *et al*. Also, using and PI/P controller for the primary and secondary controller has shown a stable response with no significant overshoot compared to the PI/PI controller used by Hurt *et al.*

The cascade controller had a more stable response with lower amplitude and lower frequency than the single controller despite the fast response. Such fluctuations are a result of the chilled water flow rate fluctuations that have a direct impact on the system's gains. From the CHW-flow rate trends, the cascade controller stabilized the valve response using the inner loop, thus, reducing the valve hunting behavior and lowering the overall amplitude. A lower frequency is relevant as it can increase the valve life span [24]. Also, a lower amplitude can lead to potential cost savings associated with a lower cooling load fluctuation.

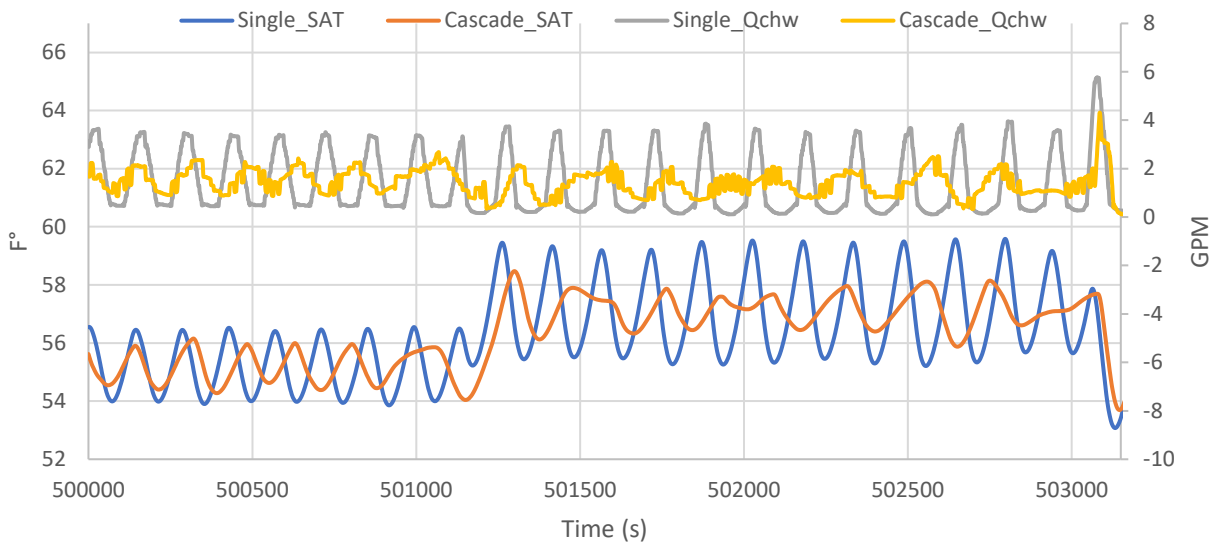


Figure 4-9 Cascade and single controller performance for T_{SA} set point step change under low load conditions

On the other hand, when a step change of DP from 17 PSI to 10 was induced, both controllers maintained a stable supply air set point temperature. Similar to Figure 4-9, the cascade controller maintained a more stable supply of air temperature with lower amplitude and lower frequency than the single controller, as shown in Figure 4-10. The cascade control stability under DP changes suggests its ability to eliminate the effect of gains changes from the chiller water loop.

As different AHUs have dynamic changes in cooling load, the tertiary pump operation changes dynamically to meet these changes, which results in DP changes. This makes cascade control a better performing option for multiple AHUs sharing one chiller water loop as it can eliminate system disturbance due to DP fluctuations.

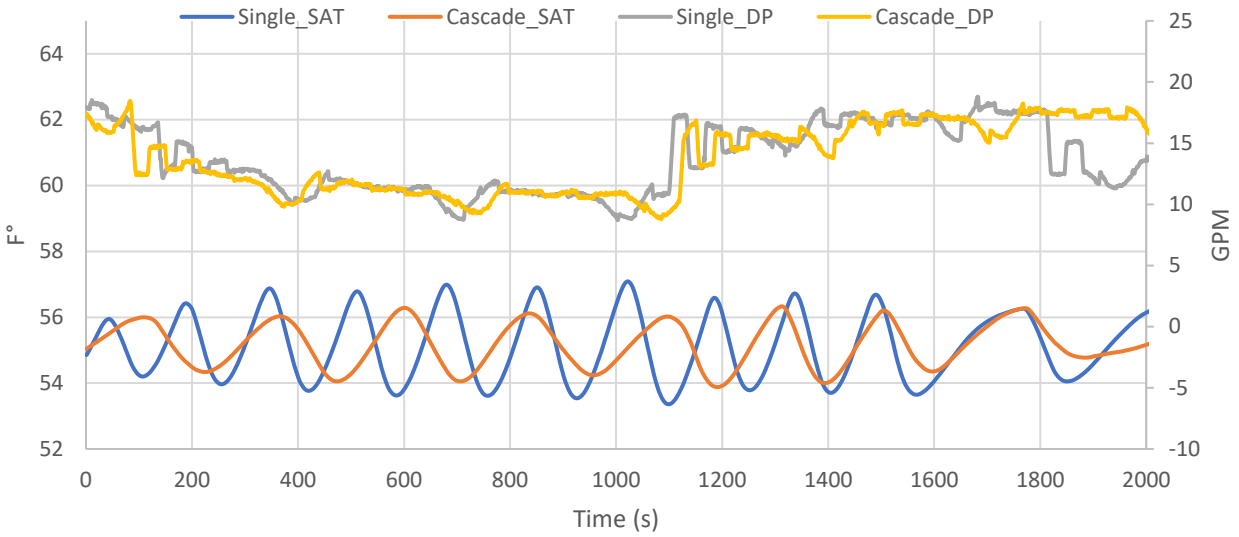


Figure 4-10 Cascade and single controller performance for DP step change under low load conditions

4.2.2 Operation under High Load Condition

When operating under high load (design conditions), cascade control has significantly better stability than the single controller. Like the low load response, the stability of T_{SA} is attributed to the stability of the chilled water flow rate measured by the VFM. Consequently, resulting in a stable valve actuation that reduces the hunting behavior. However, the frequency of chilled water flowrate is higher than that of the single controller, caused by the fast inner loop response. Without the faster inner loop, the performance will be unstable, resulting in a higher deviation from the T_{SA} set point [34, 39].

Same observations to Figure 4-10 were obtained from Figure 4-11; DP change didn't significantly impact T_{SA}. However, unlike the DP stability shown in Figure 4-12 during both the single and the cascade controller testing, the cascade testing experienced DP fluctuations. This is because the instability of the tertiary pump causes the latter during the testing. Consequently, resulting in T_{SA} fluctuations as compared to a stable single T_{SA}. This behavior has further

supported the relative stability of cascade control under unstable chiller water loops. If the same instability were presented for the single controller, higher fluctuations would be observed than in the cascade controller.

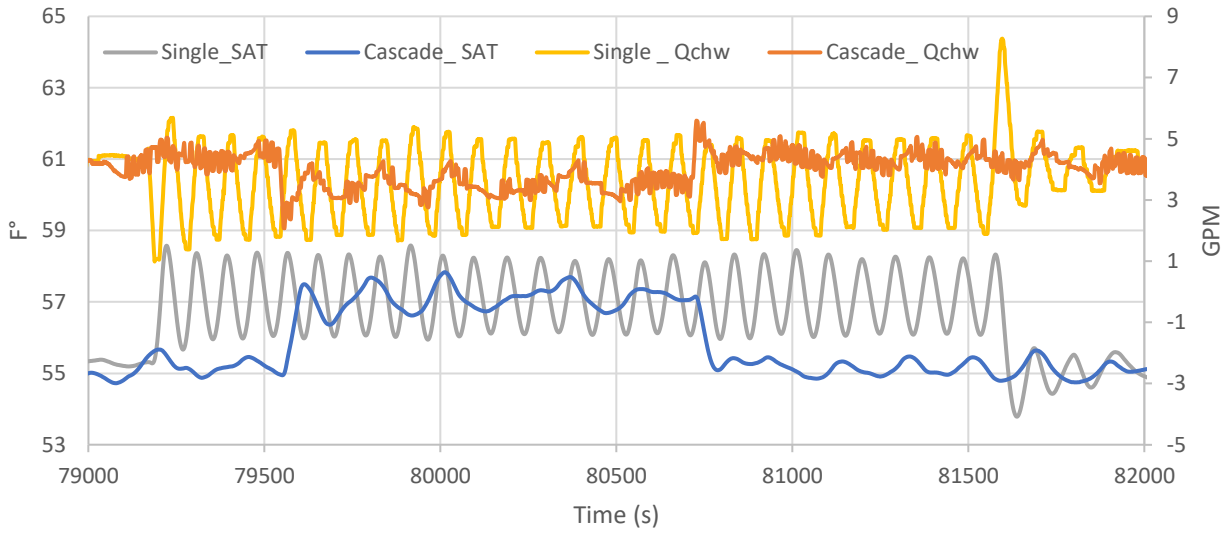


Figure 4-11 Cascade and single controller performance for T_{SA} step change under high load conditions

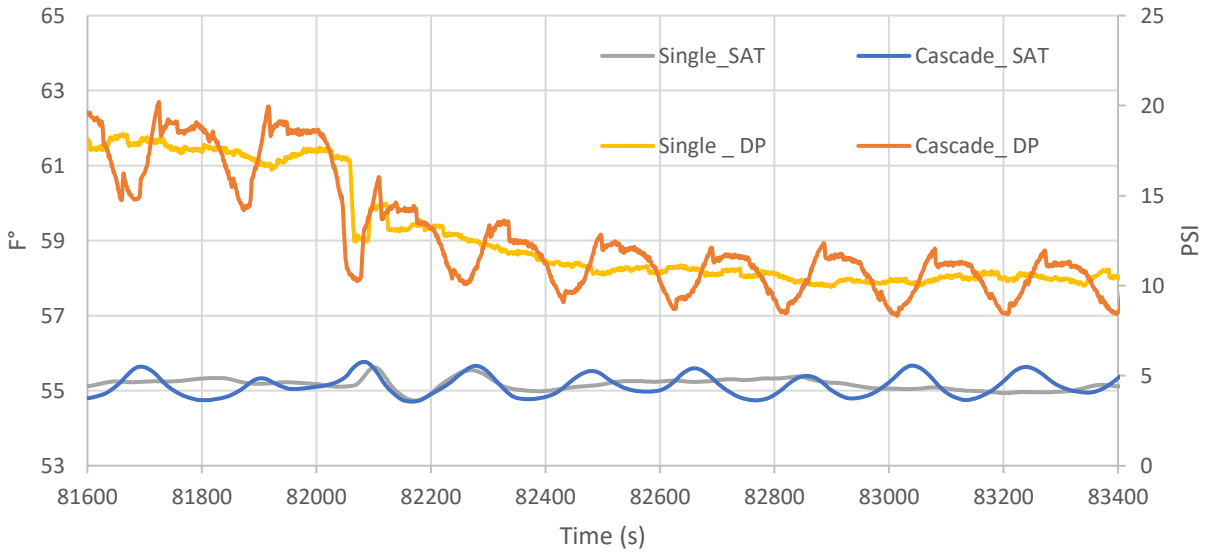


Figure 4-12 Cascade and single controller performance for DP step change under high load conditions

Table 4-2 Mean values and uncertainty analysis for each test 2 study cases

Controller type	Condition	Average T_{SA} (F°)	Standard deviation (± F°)	Standard deviation Error (%)	Frequency (Hz)	Frequency Error (%)
Single	Low	57.133	1.392	150.356	0.006	100.000
Cascade	Low	57.169	0.556		0.003	
Single	High	57.118	0.800	145.624	0.012	140.000
Cascade	High	57.119	0.326		0.005	

Overall, cascade control had better performance when using VFM than the traditional single controller. The use of CHW-VFM has allowed for inner loop chilled water flow measurement to stabilize the valve response under low and high conditions. Despite the nonlinearities at valve positions -shown in Figure 4-4, the inner controller compensated for them, resulting in a stable TSA close to the reference set point.

In addition, the VFM was modeled based only on valve position gain changes, excluding the DP gain changes. However, despite the DP gain changes when inducing a DP step change, the VFM operation maintained a stable valve response under very low DP values (10 PSI) -traditionally tuned at 17PSI. This proposes that cascade control is a better option for the chiller water loop shared by multiple AHUs because the system's stability won’t be affected by the loop’s changing loads.

This study has shown that even when a single controller is precisely tuned, the tuned cascade controller will have superior performance. Compared to a single controller, cascade control lowered TSA fluctuations by 150% in low and 145% in high conditions. It also lowered fluctuation frequency by 100% in low and 140% in high conditions. It's no doubt the cascade performed better in high conditions because it was initially tuned at design conditions (High loads). This suggests that the integration of CHW-VFM with the cascade control can cover a larger operating range without requiring seasonal gain resets, thus, reducing maintenance costs. In addition, the overall layout shown in Figure 3-4 can be implemented using the valve's empirical value with no physical sensors needed, which reduces the initial installation cost for new efficient systems.

4.3 Outdoor Air VFM

Test 2 was implemented during the month of December. That month provided a large range of temperature difference ΔT ranging from 0 F° to 50 F°. The data collected in test 2 was for one month, shown in Figure 4-13. A week was also recorded to study the feasibility of implementing a VFM with smaller sample size. The OA ratio was estimated using the energy balance Equation 9 and measured using a physical flow meter (duct traverse).

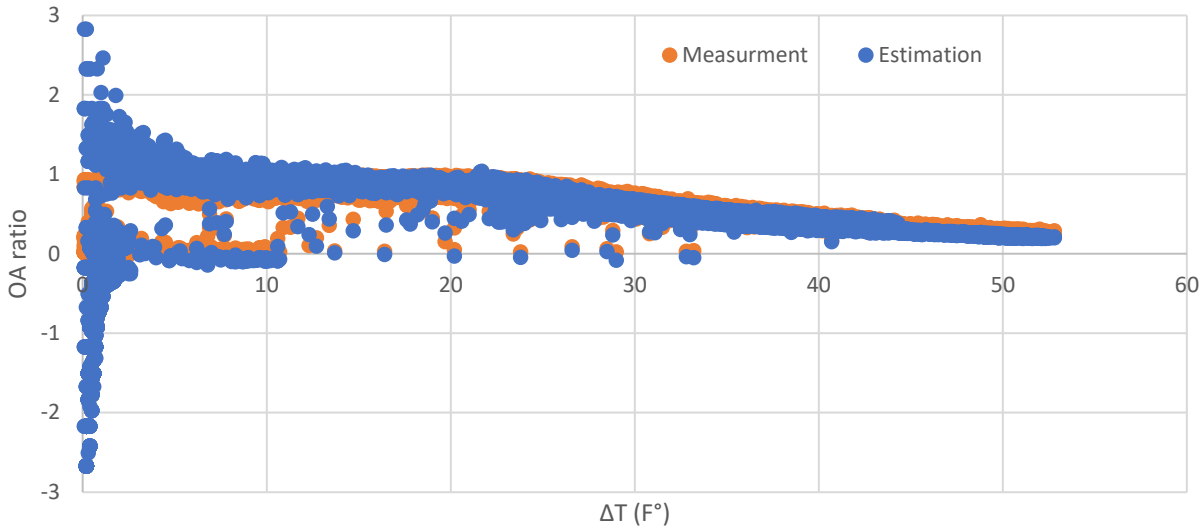


Figure 4-13 Estimation and measurement of outdoor air vs. ΔT for one-week sample size

From Figure 4-13, we can see that at low ΔT values, the estimation values are random and not accurate readings. Other studies suggest that Equation 9 is only accurate for large ΔT values [5]. The variation of outdoor air ratio results from changing damper positions under normal operation. Therefore, it is important to operate a full range of damper positions throughout the test to capture a full range of outdoor air ratios.

To further understand how the ΔT affects the estimation compared to the measured ones, the data collected was separated into five ranges of ΔT = 10 F°. However, the first region had a ΔT range of 6F°– 10F° because, for ΔT values lower than 6, the error becomes larger than 10%. For all regions, the trendline's slope of OA ratio measurement vs. estimation was always larger than 0.9, which supports the accuracy of the OA-VFM relative to the physical sensor.

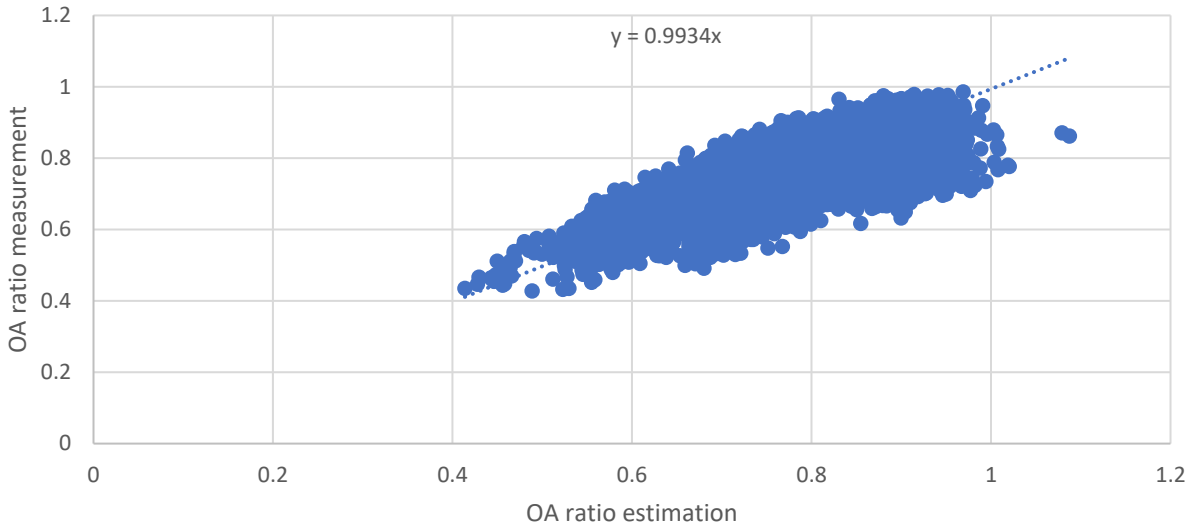


Figure 4-14 OA ratio measurement vs. estimation for ΔT = 20F° – 30F°

Table 4-3 Mean relative error values of the different ΔT ranges for the one-month sample size

One Month Sample Size	
Range of ΔT (F°)	Mean Absolute Error (%)
6 – 10	± 5.79
10 – 20	± 5.01
20 – 30	± 7.15
30 – 40	± 7.24
40 – 50	± 7.18

The five regions were analyzed for relative error, presented in Table 4-3. As ΔT gets larger, the accuracy of the OA estimation gets bigger. The average error of each region was less than 8% for

all ranges. Despite some ranges having a higher error percentage than the others, the error percentage is still relatively low to include that ΔT range in implementing the OA-VFM.

The same analysis was conducted for the one-week sample size, and Figure 4-15 was obtained. Despite the lower error associated with increased ΔT, a smaller sample size resulted in a higher relative error. Table 4-4 shows that the mean relative error of each region is larger than 20%. This suggests that to implement an OA-VFM, one-month data is required for accurate readings. Overall, the suggested minimum ΔT value is 6 F° with for an error of less than 8%

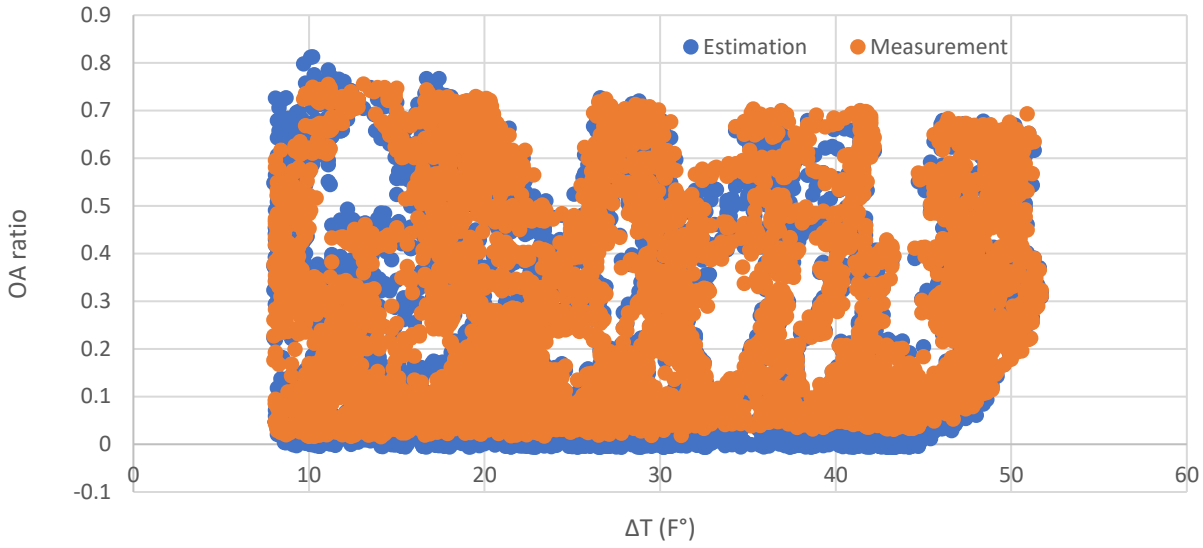


Figure 4-15 Estimation and measurement of outdoor air vs. ΔT for one-week sample size

Table 4-4 Mean relative error values of the different ΔT ranges for the one-week sample size

One Week Sample Size	
Range of ΔT (F°)	Mean Absolute Error (%)
6 – 10	± 33.8
10 – 20	± 26.4
20 – 30	± 19.8
30 – 40	± 20.2
40 - 50	± 21.2

Moreover, it was observed in Figure 4-16 that at a temperature difference higher than 20 F°, the precision of the physical flow meter decreases. As seen in Table 4-3 and Table 4-4, this lower precision has caused a higher relative error with increasing ΔT, unlike what the model suggests for values above 30 F°. Due to low ambient temperatures, the physical meter precision is affected by larger temperature drifts in the hot-wire anemometer [7]. Thus, this suggests that the physical meter measurements are not true at all ranges. Overall, implementing an OA-VFM won't be prone to reading errors under harsh weather conditions.

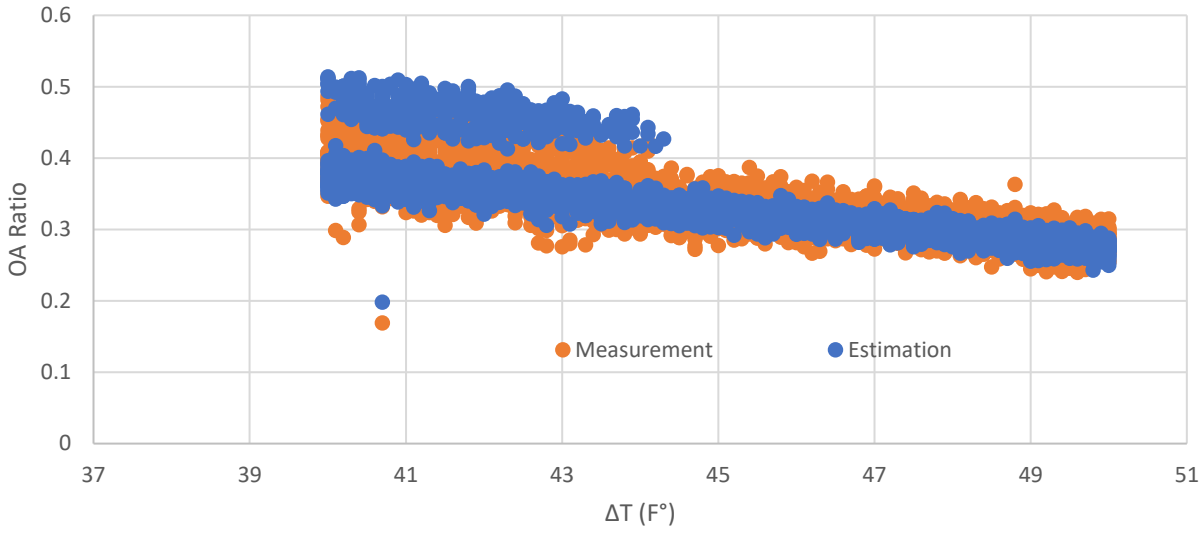


Figure 4-16 Estimation and measurement of outdoor air ratio for ΔT (F°) = 40 - 50

4.3.1 OA ratio vs. damper position

As OA ratio estimation was established for a minimum ΔT value of 6 F°, step 3 of this study includes the correlation of OA ratio vales with damper position to implement an OA-VFM that works as a function of damper position. As such, test 4 measured the OA ratio for different OA damper positions. In theory, OA airflow should change with damper position step changes, resulting in a proportional relationship. However, as shown in Figure 4-17, step changes didn't always have a proportional OA ratio response. This suggests that other factors are influencing the flow of OA at different damper positions.

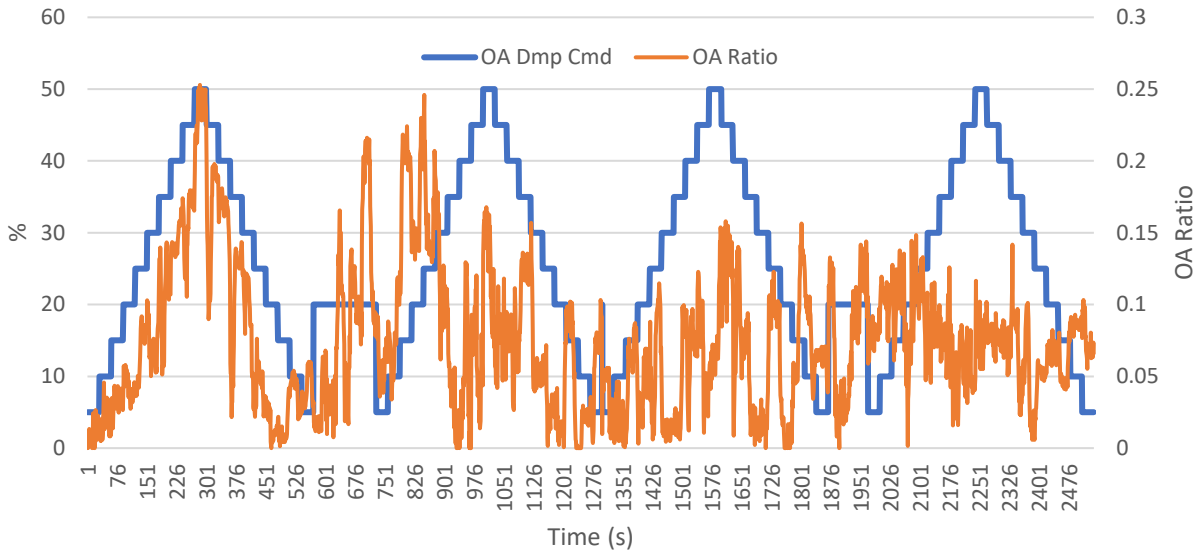


Figure 4-17 OA damper position and OA ratio values

It was found that building pressure variation directly impacts the mixing chamber pressure, which consequently influences the flow of outdoor air at different damper positions [29, 30, 35]. As a result, test 4 was conducted to verify this theory. Maintaining a constant airflow is associated with a stable chamber pressure due to a steady mass flow rate across the chamber. Figure 4-18 shows that when the system's airflow is maintained at a constant value to maintain a steady mixing chamber pressure, OA airflow is proportionally changing with the damper positions at a steady rate. Consequently, the OA ratio can be correlated as a damper position (x) function, as presented in Figure 4-19.

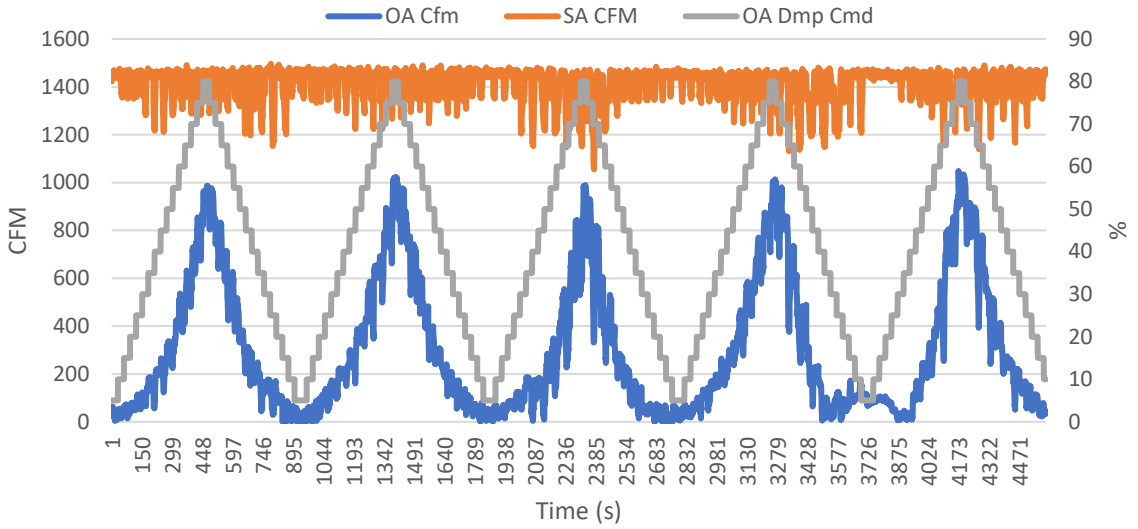


Figure 4-18 OA damper position and OA ratio values under constant systems airflow rate

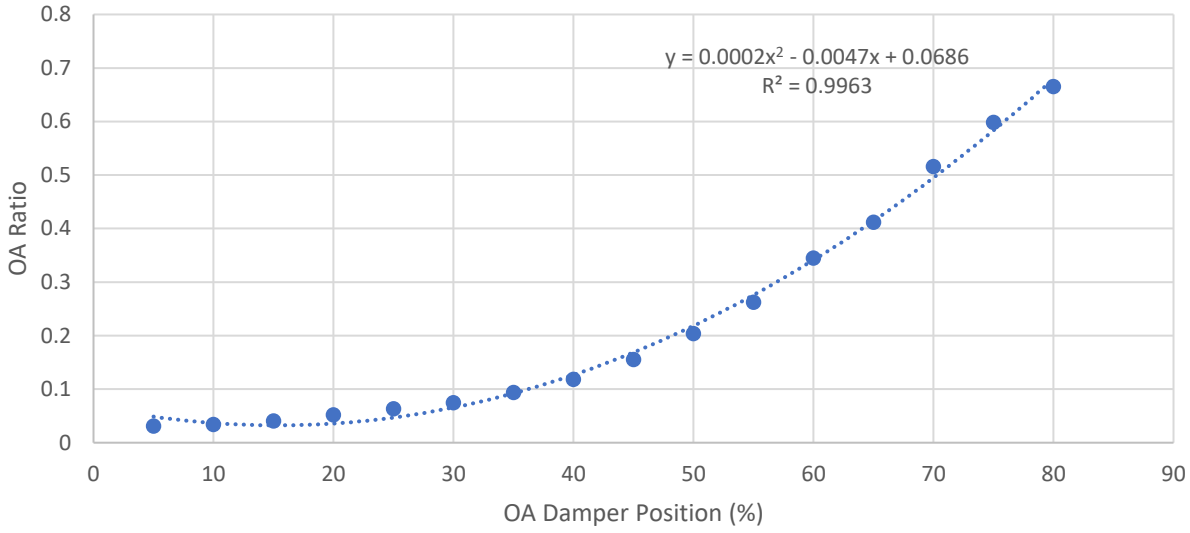


Figure 4-19 OA ratio vs. damper position

Even though a steady airflow rate across the mixing chamber gives stable pressure, different systems' airflow rates will result in different chamber pressures. The latter results from varying DP values associated with different fan speeds according to the fan's head curve.

Due to time constraints associated with this study, it was infeasible to investigate methods of maintaining a constant mixing chamber pressure. The study's approach included test 4 to examine the effect of different chamber pressure on the OA ratio correlation with damper position. Using this data, we can develop a correlation of OA ratio as a function of both damper position and systems airflow rate.

Supply fan head measurements were used to model the behavior of the mixing chamber pressure during different supply airflow rates. Starting at 1800 CFM airflow rate, Figure 4-20 shows that as the flow rate decreases, the fan head measurement decreases. The fan head changes are a result of a lower fan speed. The pressure changes are proportional to the OA ratio changes.

The data also suggests an ideal chamber pressure required to provide a valid OA ratio response to changing the OA damper position. The OA ratio behavior was non-proportional for head values lower than 1.5 InWC (1200 CFM). This observation is similar to Tan *et al*., suggesting a minimum of 40% fan speed to accurately estimate return and supply airflow, which was then used to measure OA flow [30]. However, the speed of the supply fan at 1.5 InWC is 80% (48 Hz) which is different from the suggested 40% minimum because of different duct pressure setpoints. As mentioned in Chapter 3, the supply airflow rate was controlled using TB airflow setpoints and not using direct fan speed overrides to avoid duct pressure variations.

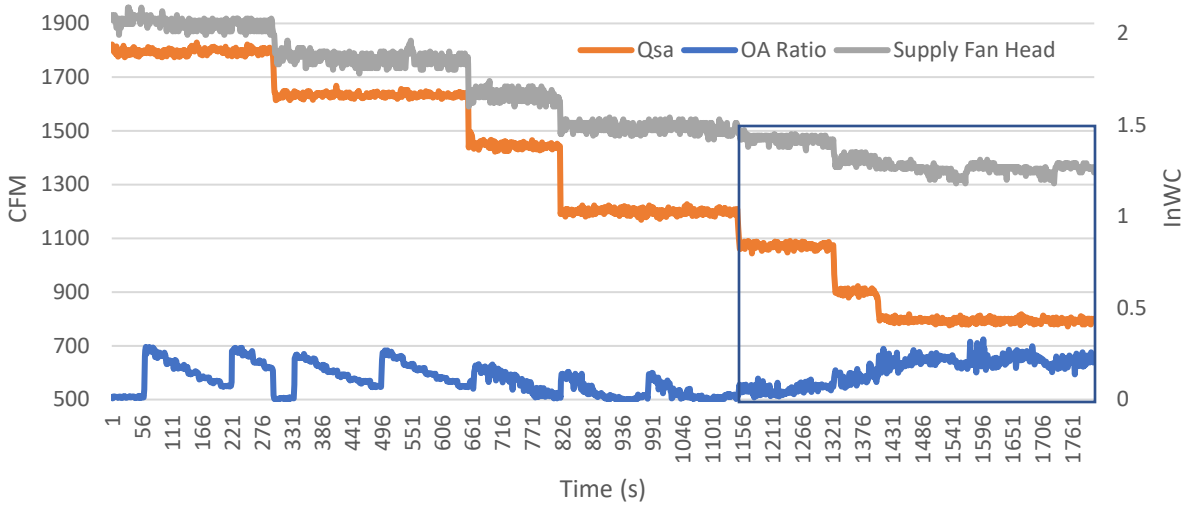


Figure 4-20 OA ratio and supply fan head at different supply airflow rates

In addition, the correlation trendlines of OA ratio to damper position were plotted for each airflow rate in Figure 4-21. It is seen that a steady proportional correlation is achieved at flow rates larger than 1200 CFM (1.5 InWC). Figures 4-20 and 4-21 validate the assumption that a steady mixing chamber pressure is needed to establish an OA-VFM correlation.

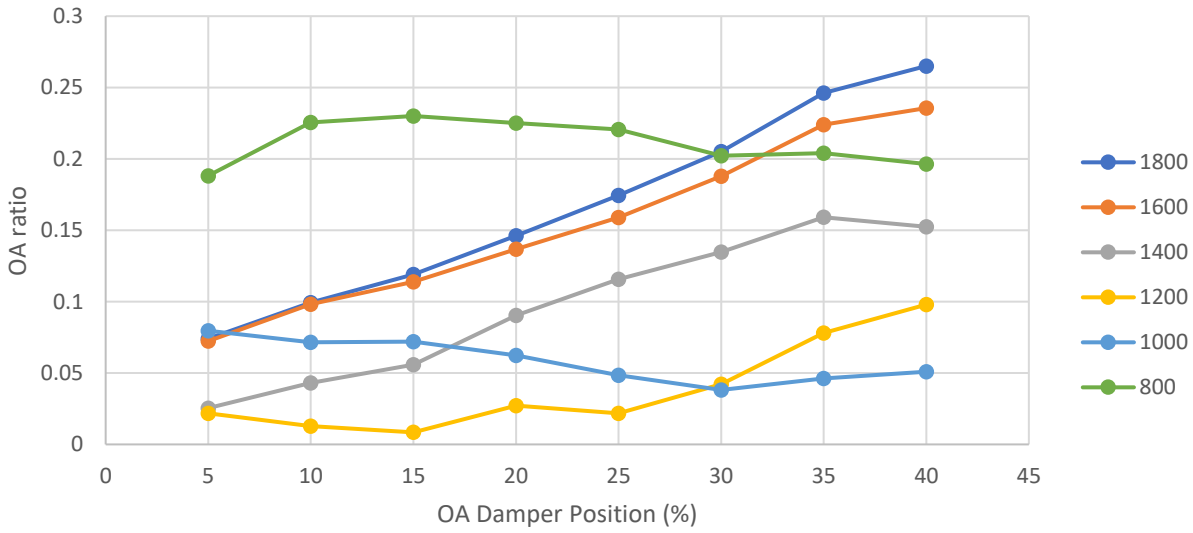


Figure 4-21 Trendlines of OA ratio correlations with damper position at different supply airflow rates

Further investigation is needed to find the ideal chamber pressure at a 1.5 InWC fan head. However, throughout the experiment, duct pressure downstream of the supply fan was constant, suggesting a decrease in upstream pressure (mixing chamber) as the fan head decreased. Therefore, it is assumed that low chamber pressure experienced at a low flow rate (<1200 CFM) can be lower than the outside pressure, leading to a constant OA airflow despite the changing damper positions.

Chapter 5 : Conclusion and Future Work

This thesis aims to investigate the application of VFM for measurements of chilled water and outdoor airflow in HVAC systems. VFM has been shown to lower initial costs associated with physical flow meters, lower maintenance costs associated with periodic sensor calibration, enhance the performance of HVAC systems, and decrease operational costs by reducing measurement errors related to faulty sensors. The thesis started by modeling a CHW-VFM as a function of DP and valve position (x) with an error of less than 5% compared to a physical flow meter. It was also shown that the physical sensor's measurement error could be more than 100% if not calibrated periodically, which decreases potential cost savings.

The CHW-VFM was also implemented in cascade control operation, enhancing the system's response using supply air temperature as reference output. Under supply air and DP disturbances, cascade control showed superiority over using a single controller by reducing fluctuation amplitude and frequency by more than 100%, as shown in Table 4-2. In addition, cascade control response to disturbances showed stable performance for both high and low operating conditions. Results suggest that cascade control can operate under a larger range of operating conditions. The latter eliminates the need for seasonal gain resets, thus, reducing maintenance costs.

Furthermore, the system's stability under disturbances when using cascade control can help lower operational costs associated with more extensive cooling load fluctuations. This performance stability is significant for AHUs sharing one chiller water loop because it helps reduce the system's instability due to chiller water loop DP changes. Moreover, the controller's stability helped reduce valve hunting and chiller water loop oscillatory flow, which reduces DP fluctuations within the loop.

The second part of the thesis implemented an OA-VFM using temperature readings from the building automation system. The VFM relied on an energy balance Equation 9 to compute the outdoor air ratio. It was found that a minimum ΔT of 6 F° is required for a correct OA ratio estimation with a relative error of less than 8%. Also, a minimum of one-month sample size is necessary to ensure low relative error compared to using a one-week sample size. The mean relative error associated with the one-week and one-month sample size is 24.28% and 6.47%.

The investigation showed the ability to correlate OA ratio as a function of OA damper position if mixing chamber pressure is maintained steadily. The results suggest an ideal mixing chamber pressure to maintain a steady proportional OA intake at changing damper positions.

Further investigation is needed to thoroughly understand the cascade control effect on the component's behavior of the overall system. For example, this study didn't investigate the potential performance benefits of different PI/P controller settings. As for the OA-VFM, an investigation should be implemented to understand the correlation between the mixing chamber pressure and the OA ratio as a function of damper position.

Moreover, this study presented the robustness of using a virtual meter instead of a physical meter. However, despite the low absolute error values for both the CHW and OA virtual meter, an uncertainty investigation should be implemented to study the effect of such error on potential cost savings. Such analysis should compare the error impact of the VFM, and the measurement errors associated with physical meters.

References

1. Miranda, L. *Clean energy conundrum: A/C units contribute to climate change but are essential for those suffering its effects*. 2021; Available from: https://www.nbcnews.com/business/business-news/clean-energy-conundrum-c-units-contribute-climate-change-are-essential-n1275928.
2. Armstrong, M. *Air Conditioning Biggest Factor in Growing Electricity Demand*. 2020; Available from: https://www.statista.com/chart/14401/growing-demand-for-air-conditioning-and-energy/.
3. Anderson, L. *How is the HVAC Industry Addressing Climate Change and Sustainability?* 2020; Available from: https://www.hvacinformed.com/insights/hvac-industry-addressing-climate-change-sustainability-co-1570804656-ga-co-1581682229-ga-co-1592321964-ga-co-1598629327-ga-off.1601288089.html.
4. *Improving Indoor Air Quality*. Available from: https://www.epa.gov/indoor-air-quality-iaq/improving-indoor-air-quality.
5. *Building Re-Tuning Training Guide: AHU Minimum Outdoor Air Operation*. Re-tuning Commercial Buidlings.
6. *Duct traversal airflow measurement*. Available from: https://www.fluke.com/en-us/learn/blog/hvac/duct-traversal-airflow-measurement#:~:text=A%20duct%20traverse%20consists%20of,%2C%20reference%20this%20airflow%20guide).
7. Lu, X., et al., *A novel simulation-based framework for sensor error impact analysis in smart building systems: A case study for a demand-controlled ventilation system.* Applied Energy, 2020. **263**: p. 114638.

8. Sane, H., C. Haugstetter, and S. Bortoff. *Building HVAC control systems-role of controls and optimization*. in *2006 American Control Conference*. 2006. IEEE.

9. *Low Temperature Air Distribution* 2019; Available from: https://blog.priceindustries.com/low-temperature-air-distribution#:~:text=The%20current%20standard%20supply%20air,water%20systems%20and%20chiller%20efficiencies.

10. Li, H., D. Yu, and J.E. Braun, *A review of virtual sensing technology and application in building systems.* Hvac&R Research, 2011. **17**(5): p. 619-645.

11. Song, L., G. Wang, and M. Brambley, *Uncertainty Analysis for a Virtual Flow Meter Using an Air-Handling Unit Chilled Water Valve.* HVAC and R Research, 2013. **19**.

12. Wang, K.P.G. and P.J. Varona, *Improving Valve Operation Using Cascade Control in Single Zone Air Handling Units.*

13. Borggaard, J., et al. *Control, estimation and optimization of energy efficient buildings*. in *2009 American Control Conference*. 2009. IEEE.

14. *The 101s: Intro to VAVs*. 2018; Available from: https://www.kmccontrols.com/blog/the-101s-intro-to-vavs/#:~:text=VAV%20stands%20for%20Variable%20Air,heat%20or%20cool%20a%20space.

15. Aktacir, M.A., O. Büyükalaca, and T. Yılmaz, *Life-cycle cost analysis for constant-air-volume and variable-air-volume air-conditioning systems.* Applied energy, 2006. **83**(6): p. 606-627.

16. Bae, Y., et al., *Sensor impacts on building and HVAC controls: A critical review for building energy performance.* Advances in Applied Energy, 2021. **4**: p. 100068.

17. Doumiati, M., et al. *Virtual sensors, application to vehicle tire-road normal forces for road safety*. in *2009 American Control Conference*. 2009. IEEE.

18. Li, H. and J.E. Braun, *Decoupling features and virtual sensors for diagnosis of faults in vapor compression air conditioners.* International Journal of Refrigeration, 2007. **30**(3): p. 546-564.

19. Swamy, A., L. Song, and G. Wang, *A Virtual Chilled-Water Flow Meter Development at Air Handling Unit Level.* ASHRAE Transactions, 2012. **118**(1).

20. McDonald, E. and R. Zmeureanu, *Development and testing of a virtual flow meter tool to monitor the performance of cooling plants.* Energy Procedia, 2015. **78**: p. 1129-1134.

21. Zhao, X., M. Yang, and H. Li, *Development, evaluation, and validation of a robust virtual sensing method for determining water flow rate in chillers.* HVAC&R Research, 2012. **18**(5): p. 874-889.

22. *P, PI, and PID Controllers*. Available from: https://www.javatpoint.com/control-system-p-pi-and-pid-controller.

23. Phalak, K. and G. Wang. *Performance comparison of cascade control with conventional controls in air handling units for building pressurization*. in *ASHRAE Winter Conference. Orlando, FL. January*. 2016.

24. Price, C. and P. Bryan Rasmussen PhD, *HVAC nonlinearity compensation using cascaded control architectures.* ASHRAE Transactions, 2015. **121**: p. 217.

25. Hurt, R., G. Wang, and L. Song, *Experimental Validation of Cooling Coil Control Valve Performance with Cascade Control.* ASHRAE Transactions, 2020. **126**(2).

26. Tianyi, Z., M. Liangdong, and Z. Jili, *An optimal differential pressure reset strategy based on the most unfavorable thermodynamic loop on-line identification for a variable water flow air conditioning system.* Energy and Buildings, 2016. **110**: p. 257-268.
27. *Standard 62.1 -Ventilation for Acceptable Indoor Air Quality*. 2019, ASHRAE.
28. Fisk, W.J., et al., *Measuring rates of outdoor airflow into HVAC systems.* 2002.
29. Phalak, K. and G. Wang, *Minimum outdoor air control and building pressurization with lack of airflow and pressure sensors in air-handling units.* Journal of Architectural Engineering, 2016. **22**(2): p. 04015017.
30. Tan, H. and A. Dexter, *Estimating airflow rates in air-handling units from actuator control signals.* Building and environment, 2006. **41**(10): p. 1291-1298.
31. Wang, G., et al., *Investigations on a virtual airflow meter using projected motor and fan efficiencies.* HVAC&R Research, 2014. **20**(2): p. 178-187.
32. Cotrufo, N. and R. Zmeureanu, *Virtual outdoor air flow meter for an existing HVAC system in heating mode.* Automation in Construction, 2018. **92**: p. 166-172.
33. *Valve Positioners*, in *Basic Principles of Control Valves and Actuators*. Control Automation.
34. Elliott, M.S. and B.P. Rasmussen, *On reducing evaporator superheat nonlinearity with control architecture.* international journal of refrigeration, 2010. **33**(3): p. 607-614.
35. Curtiss, P. and J. Kreider, *Laboratory tests of the nonlinearity of outdoor air percentage as a function of damper position and induced inlet pressure.* ASHRAE Transactions, 1992. **98**(Pt 1).
36. *Standard 55 -Thermal Environmental conditions for Human Occupancy*. 2020, ASHRAE.

37. *ASHRAE Handbook*. 2021: ASHRAE.

38. Heath, H. *What is control valve dead band?* 2020; Available from: https://www.rampfesthudson.com/what-is-control-valve-dead-band/.

39. Lee, Y., S. Park, and M. Lee, *PID controller tuning to obtain desired closed-loop responses for cascade control systems.* IFAC Proceedings Volumes, 1998. **31**(11): p. 613-618.